Department of Construction Sciences
Division of Solid Mechanics

ISRN LUTFD2/TFHF-06/5127-SE(1-63)

Finding general guidelines for choosing appropriate cut-off frequencies for modal analyses of railway bridges trafficked by high-speed trains

Master's Dissertation by

Björn Lundin
and
Philip Mårtensson

Supervisors

Johan Kölfors, Scanscot Technology, Sweden
Håkan Hallberg, Div. of Solid Mechanics, Lund University, Sweden
Magnus Harrysson, Div. of Solid Mechanics, Lund University, Sweden

Printed by Media-Tryck, Lund University, Lund, Sweden
For information, adress:
Division of Solid Mechanics, Lund University, Box 118, SE-221 00 Lund, Sweden
Homepage: http://www.solid.lth.se

Abstract

Railways, which in the future will be trafficked by high-speed trains, are designed with respect to the dynamic responses that these trains raise. The dynamic response is normally calculated using modal superposition, based on an eigen frequency base defined by the highest frequency included, the so called cut-off frequency. A higher cut-off frequency gives more accurate results but demands a longer computational time. Because of the extensive number of dynamic analyses needed to be performed for a bridge trafficked by high-speed trains, it is desirable to minimize the frequency base and thereby receive as short computational time as possible. At the same time, the accuracy of the results must be satisfying i.e., choosing the cut-off frequency is in a sense a balance between cost and quality.

This study aims to find general guidelines for choosing an appropriate cut-off frequency, when performing modal dynamic analyses of concrete bridges trafficked by high-speed trains. To do so, a convergence study was carried out for two types of bridges to find acceptable cut-off frequencies. With the cut-off frequency known, an attempt to find a relation between the load frequency and the found cut-off frequency was made. Also, the use of residual modes when performing modal dynamic analyses was studied, by performing the same analyses as when searching for the cut-off frequencies but with residual modes included.

The study shows that the cut-off frequency depends on which result component of the section forces chosen to be studied. For bridge 1, a long three span bridge, the analyses converged earlier when studying the bending moment than when studying the shear forces.

There are few bridges stiffer than bridge 2, a short frame bridge. A higher cut-off frequency than needed for bridge 2 is not likely to be needed when performing modal dynamic analyses on bridges. For the convergence criterion set up in this report, the analyses for bridge 2 converge when a cut-off frequency of 160 Hz was used. That is about four times the highest frequency any of the studied standardized high-speed trains generates. The results also show that the analyses for each bridge converge at the same cut-off frequency, independent of which standardized train load used in the analyses. This leads to the conclusion that a cut-off frequency higher than 160 Hz is most likely never needed for any bridge and standard vehicle combination.

Using residual modes proved to have a big impact on the analyses performed on bridge 2 but smaller on bridge 1. For bridge 2, the cut-off frequency was lowered 50 % when a residual mode was used. For the residual modes to be a powerful tool and making better analyses, the user's knowledge on how to generate an adequate residual mode is essential. Guidelines are presented in this paper on how to generate adequate residual modes.

The results also show that, studying the effective mass is a conservative method when defining a cut-off frequency for bridges, if assuming an un-deformable ground.

Acknowledgements

This Master Thesis was carried out from May to November in 2006 for Scanscot Technology with supervision from the Division of Solid Mechanics at Lund Institute of Technology.

We would like to thank Scanscot Technology for giving us the opportunity to carry out this project. We would also like to thank everyone at Scanscot for a pleasant time and for helping us with all the small things that seemed trivial but helped us advance in our work. We would especially like to thank Johan Kölfors, our supervisor at Scanscot and the initiator of this thesis. We would like to thank him for his never-ending patience, for spending too much time at our desk instead of his own and his infinite many good ideas helping our work to proceed.

We are also grateful for all the help from our supervisors at the Division of Solid Mechanics, Håkan Hallberg and Magnus Harrysson. The help with the research of literature and all the important feedback throughout this project has been very useful to us.

Finally, we would like to thank everyone else that has giving us viewpoints of the project and to everyone that has supported us in this project.

Lund, November 2006

Björn Lundin and Philip Mårtensson

Contents

1 Introduction

1.1 Scanscot Technology

Scanscot Technology has been active in two major areas since it was founded in 1992, development of analysis software products and consulting within civil, structural and mechanical engineering. In both areas advanced structural Finite Element Analyses (FEA) are used.

Scanscot Technology is the developer of the analysis software package BRIGADE, containing the products BRIGADE/Standard and BRIGADE/Plus. Both programs are based on an integrated implicit solver from ABAQUS. The software is mainly developed to analyse bridges and other civil structures but can be used for other purposes as well. For further information, visit www.scanscot.com.

1.2 Background to assignment

Railways, which in the future will be trafficked by high-speed trains, are designed with respect to the dynamic responses that these trains raise. The dynamic response is normally calculated using modal superposition analysis, based on an eigen frequency base defined by the highest frequency included i.e. the cut-off frequency. The more complete the frequency base is chosen, the higher the accuracy of the results will be. On the other hand, a larger frequency base demands longer computational time because there will be more modes to include in the superposition. At the same, the computational time will increase due to the need of shorter increments in order to dissolve the high frequency modes.

The total computational time is extensive since each bridge must undergo one analysis for each one of the ten high-speed trains HSLM-A1 - HSLM-A10 defined in the Swedish design code for railway bridges [2]. For each bridge it is not known, for which train type the greatest dynamic response will occur, or at what velocity it will occur. Because of the extensive number of dynamic analyses needed to be performed for a bridge trafficked by high-speed trains, it is important to minimize the frequency base to maintain a reasonable computational time. At the same time, the accuracy of the results must be satisfying.

For many types of structures, a study of effective mass is used to select the cut-off frequency when performing a modal dynamic analysis e.g. an earthquake analysis. In such analyses, the cut-off frequency is chosen by studying the sum of the effective mass of the participating modes. Common praxis in such analyses is to include enough modes until 90 % of the total mass is excited. For most analyses of bridges trafficked by high-speed trains, the soil is assumed to be un-deformable. Since bridges normally have a considerable part of the total mass located in the supports a relative high cut-off frequency is needed to excite 90 % of the total mass. Therefore, for most bride structures, effective mass is not an appropriate method when trying to find a cut-off frequency.

1.3 Problem formulation

Is there a way to define practical guidelines when trying to determine a cut-off frequency for modal dynamic analyses of bridges trafficked by high-speed trains?

1.4 Objectives

By studying two types of bridges and the properties of high-speed trains, this report aims to find guiding principles for choosing a cut-off frequency when performing modal dynamic analyses of concrete bridges. The bridges are modelled in a 3-D environment using BRIGADE/Plus.

1.5 Limitations

To verify the results, analyses have to be made for some different types of bridges. Because of the long computational time there are some limitations for the verification:

- Verification will only be made on two types of bridges.
- Only the worst-case trains, i.e. the trains that generate the greatest dynamic responses, will be tested on each bridge.
- Only shear forces and bending moments will be studied. A full dynamic bridge analysis also requires studies of vertical accelerations but will not be considered in this study since the Swedish bridge design code [2] already defines the cut-off frequency for such analyses.
- Track irregularities and interaction between rail and train wheels will not be considered in this study. This is in accordance with specification for short and medium span bridges found in [2].

1.6 Method

The approach of this study is defined in three steps:

1. An attempt to find the cut-off frequency through a convergence study.

2. An attempt to find a relation between the cut-off frequency and the load properties.

3. An investigation to determine whether the use of residual modes can be helpful when attempting to find a satisfying cut-off frequency.

2 Theory of dynamic analysis using FEM

2.1 FEM

Differential equations, set up to describe physical phenomena that are too complicated to be solved analytically, can be approximately solved numerically. The most widely used method to solve systems of differential equations numerically is the Finite Element Method (FEM) [1].

With a complete model of a structure's geometry, material properties, boundary conditions and the loads applied on it, a Finite Element Analysis (FEA) can produce several results. The load applied on the structure, can be of different kinds such as: heat, force, electric current and many other. Additionally**,** FEM can be used to calculate the natural frequencies and the modal shapes of a structure.

The global structure of interest in a finite element analysis is divided into smaller parts/elements with corresponding nodal points. The equilibrium in these nodes can be described by simple equations. These equations are usually combined and written with the standard FE-formulation

$$\mathbf{M\ddot{u} + Ku = f} \tag{2.1}$$

where **K** is the global stiffness matrix including the geometry and material property of the structure, **u** the displacement vector containing the displacements at the nodes and **ü** is the acceleration vector. **M** is the mass matrix and **f** is the external forces and boundary conditions applied at the nodal point in the structure.

When modelling the bridges in this project, shell elements have been used. Shell elements are only an approximation of the field equations and reduce a 3-dimensioned problem into a 2-dimensioned problem that can be calculated simpler. The reason why shell elements are used is that, for structures with a small thickness compared to the other dimensions, the accuracy of the solutions is often sufficient.

For shell elements, the matrices **K** and **f** are defined as

$$\mathbf{K} = \int_A \mathbf{B}^{\mathrm{T}} \tilde{\mathbf{D}} \mathbf{B} dA \tag{2.2}$$

$$\mathbf{f} = \mathbf{f_b} + \mathbf{f_I} = \oint_L \mathbf{N}^{\mathrm{T}} \left(V_{nz} + \frac{dM_{nm}}{dm} \right) dL - \oint_L (\nabla \mathbf{N})^{\mathrm{T}} \mathbf{n} M_{nn} dL + \int_A \mathbf{N}^{\mathrm{T}} q dA \tag{2.3}$$

where $\mathbf{f_b}$ represents the forces at the boundary conditions and $\mathbf{f_I}$ represents the internal forces. **N** is the shape function of the element and **B** is defined as $\mathbf{B} = \nabla \mathbf{N}$. **D** is the constitutive matrix including the material properties. The shear force is in the formulation denoted as V_{nz} while the torsion moment and bending moment are denoted as M_{nm} and M_{nn} respectively. "q" is the distributed force per unit area acting on the elements and n, m and z are coordinate indexes for section/plane identified by the normal vector **n**.

Beam elements have also been used for some parts in the modelling. Since beams are dominated by the extension in the axial directions, a number of assumptions can be made. Accordingly, field equations and beam elements are therefore also just an approximation. The FE-formulation for beam elements can also be written as Equation. 2.1 but instead with the matrices **K** and **f** defined as

$$\mathbf{K} = \int_a^b \mathbf{B}^{\mathrm{T}} EI \mathbf{B} dx \tag{2.4}$$

$$\mathbf{f} = \mathbf{f_b} + \mathbf{f_l} = \left[\mathbf{N}^{\mathrm{T}} V\right]_a^b - \left[\frac{d\mathbf{N}^{\mathrm{T}}}{dx} M\right]_a^b + \int_a^b \mathbf{N}^{\mathrm{T}} q dx \tag{2.5}$$

The term EI is called the bending stiffness. If it varies over the cross-section, it can be defined as

$$EI = \int_A Ez^2 dA \tag{2.6}$$

V, M and q are still the notations for shear force, moment and distributed load. E is the Young's Module and z is the distance from the normal plane of the beam.

2.2 Linear dynamic analysis

A dynamic analysis is more complex than a static analysis due to the time varying load/loads. At the same time the response of the structure varies in time when affected to a dynamic load. A linear static analysis results in only one solution. A dynamic analysis results in a series of solutions that correspond to the time that is chosen to be studied.

In a dynamic analysis, not only internal forces are present but also inertia forces resulting from the accelerations of the structure.

Bridges trafficked by high speed trains (speed > 200 km/h) must undergo dynamic analysis because of the risks of vibration resonance that might occur due to the high speed. Resonance of the vibrations can lead to ballast instability and exceeding of the stress limit of the bridge [3].

2.3 Dynamic load and resonance

Resonance is the consequence of a train's high speed and regularly spaced axles. The regular spacing of the axles causes a periodic load with a certain frequency *f* and time period *T*, shown in figure 2.1 (b). The relationship between the frequency *f*, the time period *T*, the velocity of the train *v* and the length of the wheel spacing *L* is shown in Equation 2.7. The similarity with a harmonic load is shown in Figure 2.1 (a).

$$f = \frac{1}{T}, \quad T = \frac{L}{v} \quad \Rightarrow \quad f = \frac{v}{L} \tag{2.7}$$

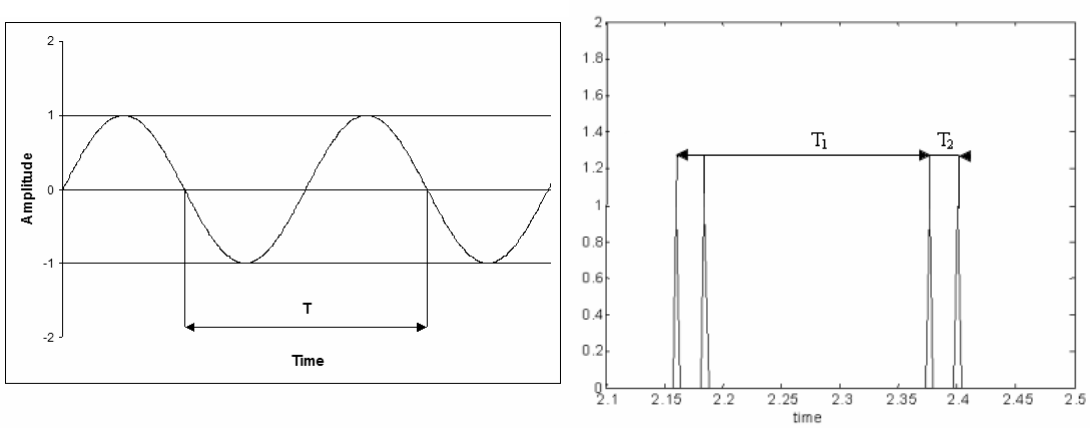

Figure 2.1: (a) *The time period T given in a harmonic load,* ***(b)*** *Two different time periods given in the periodical load from a high-speed train*

On a train set there are several repeated space lengths, see Figure 2.2, that could generate different frequencies through different time periods depending on the velocity of the train. If this load-generated frequency is equal to or close to one of the natural frequencies of the structure resonance may occur.

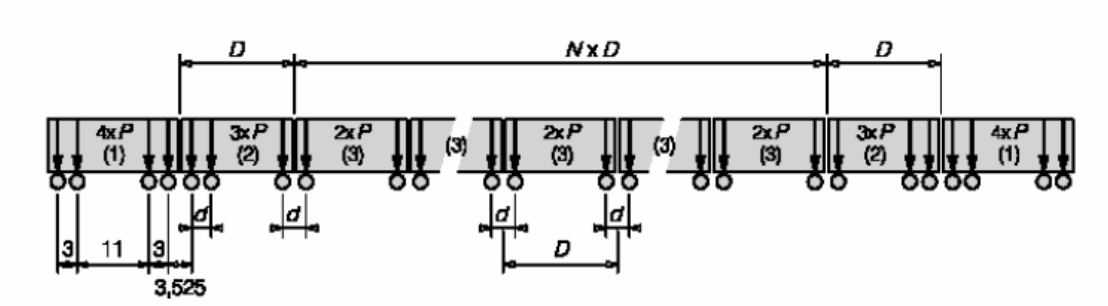

Figure 2.2*: From [2]*

2.4 Modal Analysis

The frequencies, at which vibration of the structure naturally occurs and the modal shapes, which the vibrating system takes, are properties of the system. The natural frequencies and the modal shapes of a simple system can be determined analytically. Modal analyses applied on more complex systems are often solved numerically through FEA.

2.4.1 Eigenvalue problem

The equation of motion for a freely vibrating system without damping can according to [1] be expressed:

$$\mathbf{M}\ddot{\mathbf{u}} + \mathbf{K}\mathbf{u} = \mathbf{0} \tag{2.8}$$

where **M** is the mass matrix, **u** is the displacement vector and **K** is the stiffness matrix of the system. The motion is assumed to be simple harmonic, which can be express as

$$\mathbf{u}(t) = \boldsymbol{\varphi}\sin(\omega_n t) \tag{2.9}$$

where $\boldsymbol{\varphi}$ is the amplitude of the motion, ω_n is the natural circular frequencies of vibration or eigenfrequencies of the system. Substituting Equation 2.9 and its second time derivate into Equation 2.8 gives

$$-\omega^2\mathbf{M}\boldsymbol{\varphi}\sin(\omega_n t) + \mathbf{K}\boldsymbol{\varphi}\sin(\omega_n t) = \mathbf{0} \tag{2.10}$$

which can be rewritten as

$$\left(\mathbf{K} - \omega_n^2\mathbf{M}\right)\boldsymbol{\varphi} = \mathbf{0} \tag{2.11}$$

Applying Cramer's rule [1], it can be shown that the only nontrivial solutions are possible when

$$\left\|\mathbf{K} - \omega_n^2\mathbf{M}\right\| = 0 \tag{2.12}$$

Equation 2.12 is the characteristic equation of the system and the solution gives *N* real roots of the eigenfrequencies $\omega_n^{\,2}$ for a system with *N* degrees of freedom. Each root represents the frequency of a mode of vibration possible in the system and has a corresponding mode shape vector ϕ_n. The frequency vector

$$\boldsymbol{\omega} = \begin{bmatrix} \omega_1 \\ \omega_2 \\ \vdots \\ \omega_N \end{bmatrix} \tag{2.13}$$

includes all frequencies arranged in sequence.

2.4.2 Mode superposition

The mode superposition method is used to determine the dynamic response in a linear structure where the damping can be expressed as modal damping ratios and the displacements are given by a set of *N* discrete coordinates. By solving the response for each modal coordinate and subsequently superposing the results to determine the response in the original coordinates gives the dynamic response in the structure. The basis in the mode superposition method of a dynamic analysis is to change the set of *N* coupled equations of motion into a set of *N* uncoupled equations, by normal-coordinate transformation. For more details, see [8].

After solving the eigen value problem in the previous section, the eigen frequencies ω_n and the mode-shapes ϕ_n are defined. If the structural properties are known as well, the response of the system can be calculated using a set of generalized coordinates $q_n(t)$. The response of each mode can then be determined by solving the equation

$$M_n\ddot{q}_n + C_n\dot{q}_n + K_n q_n = f_n(t) \tag{2.14}$$

where C_n is the damping and f_n is the external load. M_n, C_n, K_n and f_n are generalized and defined as:

$$\begin{aligned} M_n &= \phi_n^T \mathbf{M} \phi_n \\ K_n &= \phi_n^T \mathbf{K} \phi_n \\ C_n &= \phi_n^T \mathbf{C} \phi_n \\ f_n(t) &= \phi_n^T \mathbf{f}(t) \end{aligned} \tag{2.15}$$

The **C** matrix is defined as:

$$\mathbf{C} = \begin{bmatrix} c_1 \\ c_2 \\ \vdots \\ c_N \end{bmatrix} \tag{2.16}$$

where

$$c_n = 2\zeta m_n \omega_n \tag{2.17}$$

ω_n is the circular frequency of the mode and ζ the damping ratio.

Since all parameters in Equation 2.15 depend on the n:th mode only, there exist N uncoupled equations, one for each mode.

The total dynamic response can then be calculated by adding the contribution from all N modes:

$$\mathbf{u}(t) = \sum_{n=1}^{N} \phi_n q_n(t) \tag{2.18}$$

2.4.3 Cut-off frequency

All structures have endless many natural frequencies. A modelled structure has as many natural frequencies as there are degrees of freedom. The modes chosen to be included in the analysis must therefore be chosen wisely. If too few modes are included, the result will not be accurate [4]. If too many modes are included, the analysis will end up with an unreasonably long computational time. For every dynamic modal analysis a cut-off frequency must be chosen in such a way that both accurate results are received and computational time is minimized. The use of a cut-off frequency, which truncates the higher modes, is possible because the low-frequency-modes mainly affect the structure [4].

2.4.4 Residual modes

Residual modes compensate for the truncated modes, modes with eigen frequencies above the cut-off frequency, in the modal analysis. The modal shape and frequency depends on the frequency base chosen for the analysis. The compensation is a result of the contribution of effective mass that the residual mode brings to the modal analysis.

2.5 Study of convergence

A study of convergence can be made to decide whether a satisfying cut-off frequency has been chosen. For bridge structures, shear forces and bending moments in the superstructure are of main importance and will therefore be included in the study of convergence [2]. If all modes are considered, which is not practically possible, 100% convergence will be obtained. To shorten the computational time, a convergence criterion is set up. Convergence studies in modal analysis are difficult because the decision of including an additional mode can lead to vastly different results in the convergence study i.e. the results the analysis seemed to be aiming at could change quickly. Therefore it is difficult to determine when a certain degree of convergence is reached.

3 Method of choosing an appropriate cut-off frequency from a dynamic load study

3.1 Fast Fourier transformations (FFT)

Fourier transformations can be used to transform a time function into a function in the frequency domain. Fast Fourier transformation is a discrete Fourier transform algorithm. It computes the same results as the discrete Fourier transform but only needs N(logN) operations instead of N^2 operations for the transformation.

3.2 Theory

A simply supported beam will be used as an example to explain the idea behind the study of dynamic loads.

If a simply supported beam is subjected to a pulse force F at its centre as in Figure 3.1 and then is allowed to vibrate freely, it will eventually stop vibrate due to the inner damping of the beam, as shown in Figure 3.2. The shape and the frequency of the beam during the vibrations will correspond to the shape and frequency of the beam's first and third vertical bending modes, which is shown in Figure 3.3.

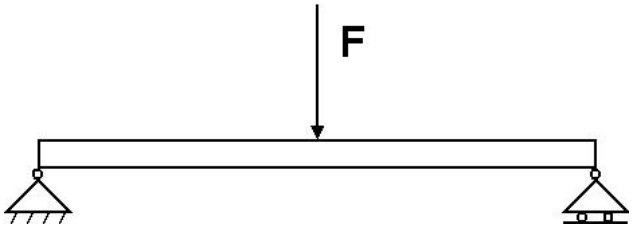

Figure 3.1: *A simply end-supported beam subjected to a vertical force at its centre.*

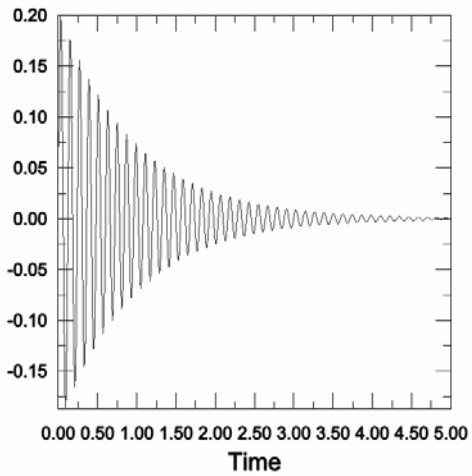

Figure 3.2: *Force F applied once at time t = 0 as demonstrated in Figure 3.1. The inner damping of the system forces the beam to stop vibrating after some time. The vertical axel shows the value of the bending moment at the centre of the beam.*

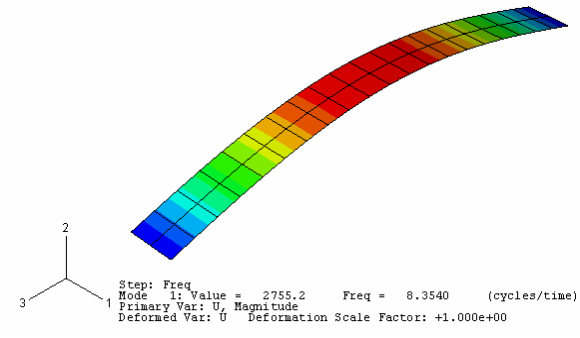

Vertical bending mode 1: 8.35Hz

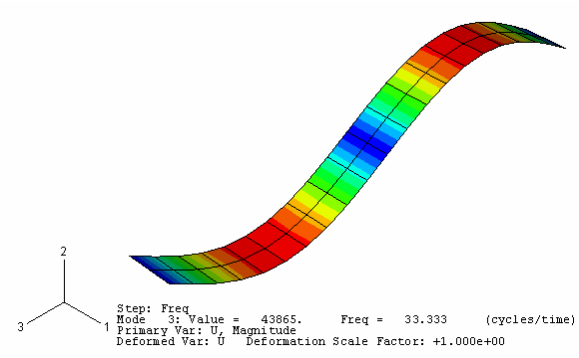

Vertical bending mode 2: 33.33Hz

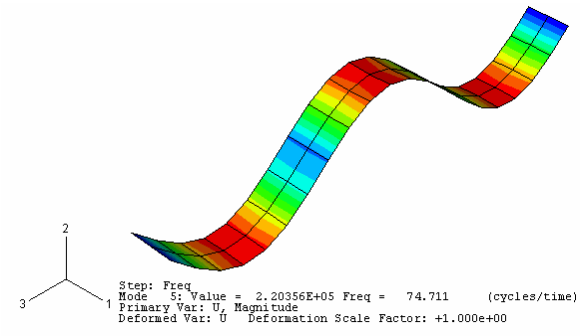

Vertical bending Mode 5: 74.71Hz

Figure 3.3: *First three vertical bending modes for the simply supported beam*

If the beam is subjected to a force at a frequency (f_F) that corresponds with one of the natural frequencies of the beam (f_n), resonance will occur ($f_F = f_n$). As a result, this causes the deflection of the beam to increase every time the force is applied. When the force is removed the vibrations of the bridge will damp out. Figure 3.4 (a) shows the time history for the bending moment at the centre of the bridge when force F is applied five times with a frequency of 8.35Hz, the same frequency as the bridge's first natural frequency. Figure 3.4 (b) reveals the time history in Figure 3.4 (a) transformed into the frequency plane through the use of Fast Fourier Transformation (FFT).

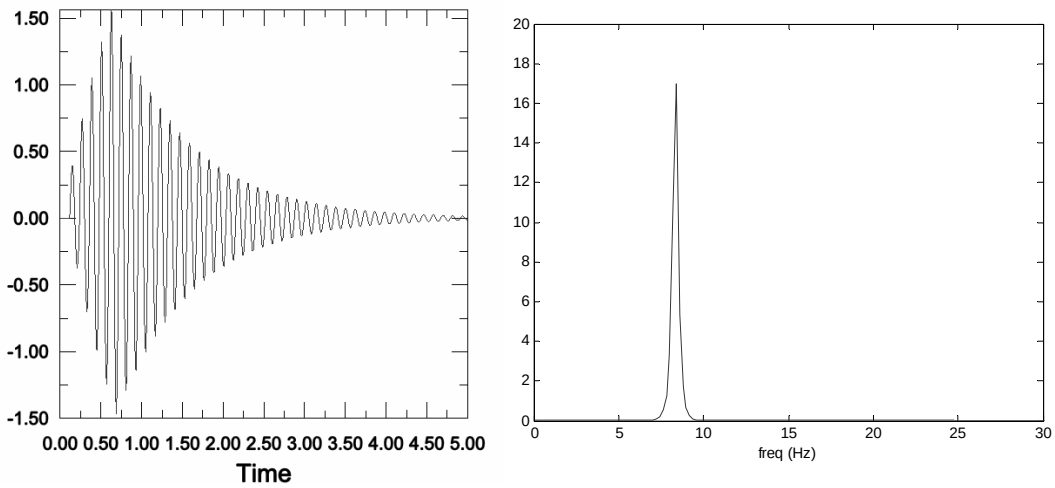

Figure 3.4: (a) *Time history for the bending moment (SM1) at the centre of the beam when force F was applied 5 times with frequency $f_F = f_n = 8.35$Hz. Cut-off frequency 10Hz.* ***(b)*** *The time history of the bending moment transformed into the frequency plane through FFT.*

The force acting at the same frequency as the beam's natural frequency denotes that every time the beam is flexed up to its highest point at the centre, the force is applied. For example, if the force F is applied with a frequency that is half the natural frequency ($f_i = f_n/2$) of the beam the force will be applied every second time the beam flexes up. This will also cause resonance but not as significant as when the force is applied at the same frequency as the bridge's natural frequency. Also, when force is applied at half the frequency, every second peak will be lower because the beam will have time to vibrate freely once before the next pulse force is applied. Figure 3.5 (a) shows the time history of the bending moment at the centre of the beam when the force F is applied at a frequency of $f_n/2$ = 4,18Hz. Notice that the maximum bending moment reaches a higher value when the force is applied with the same frequency as the bridge's natural frequency, as opposed to when it is applied with only half the frequency. Figure 3.5 (b) shows the time history of the bending moment transformed into the frequency plane through FFT.

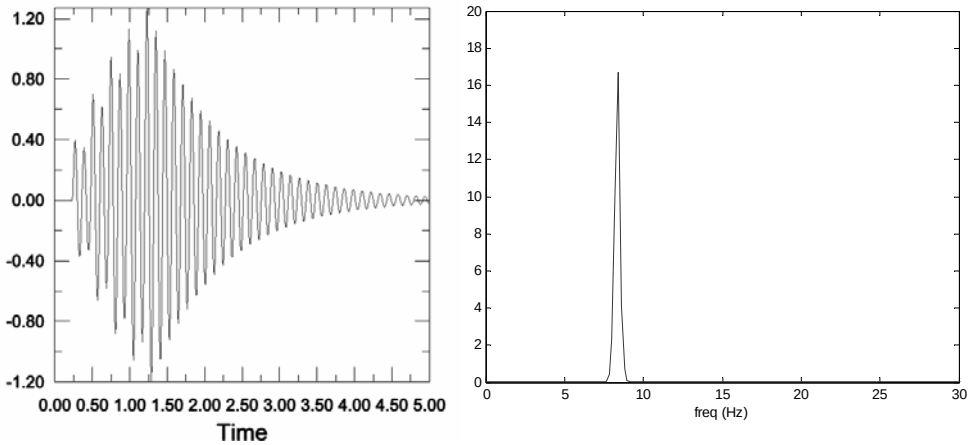

***Figure 3.5**: **(a)** Time history for the bending moment (SM1) at the centre of the beam when force F was applied 5 times with frequency $f_F = f_n/2 = 4.18$Hz. Cut-off frequency 10Hz. **(b)** The bending moment time history transformed into the frequency plane through FFT.*

With the same reasoning, resonance can be generated by applying a pulse force with a frequency that is a third, quarter, etc. of the beam's natural frequency ($f_F = f/k$, k = 1,2,3…). However, if the frequency of the force is too low (k is a large integer), the beam will have time to damp the vibrations between the time periods when the force is applied. This means that there will be no resonance.

Resonance of the beam can only occur at its natural frequencies. The frequency of the force acting on the beam, or the force's frequency divided with an integer, must correspond with one of the natural frequencies of the beam (not necessarily the first) to cause resonance. Forces acting on the beam at other frequencies are harmless, in regards to resonance. Figure 3.6 (a) shows the time history of the bending moment at the centre of the beam when force F is applied 5 times with a frequency of 20Hz. As illustrated, no resonance is present. This is further demonstrated in Figure 3.6 (b) through the absence of a peak at a specific frequency.

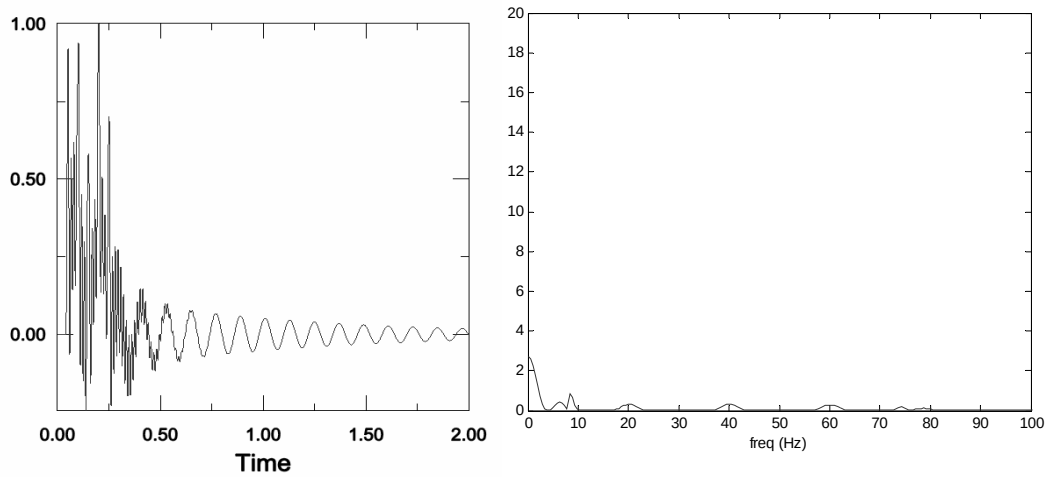

Figure 3.6: (a) *Time history for the bending moment (SM1) at the centre of the beam when force F was applied 5 times with a frequency of 20Hz. Cut-off frequency 100Hz.* ***(b)*** *The bending moment time history transformed into the frequency plane through FFT.*

For the force to be able to excite a certain eigenmode it must not only have a certain frequency ($f_F = f_n/k$, k = 1,2,3…), but also it must act on a certain point or certain points. For example, if the force F is applied as in Figure 3.1, it can excite the vertical bending modes 1 and 3 but not the mode 2. It is intuitive that the vertical force F cannot trigger modes on which the point it is acting is not moving in the force's direction.

To accelerate calculations in a modal analysis, one can choose to exclude modes that cannot be excited due to the position/positions of the force/forces applied. The same result will be obtained when the non-excited modes are included as when they are excluded. When performing a modal analysis on a simple structure, such as a beam, it may be easy to exclude some modes in the analysis. However, when performing an analysis on a more complex structure, such as a bridge subjected to a trainload, it is much more difficult to exclude modes that do not effect the results. The time needed to the selection procedure, of which eigenmodes to include, as well as the following result verification, can be just as time consuming as including all eigenmodes in the frequency base.

If a modal analysis is performed on the system in Figure 3.1, excitation of the first mode will occur. Including only the first mode in the modal analysis i.e. choosing a cut-off frequency just above 8.35 Hz may not be enough. The beam may have eigenmodes with frequencies that are integer-multiples of the frequency with which the force is applied. Figure 3.7 (a) shows the response of the same analysis as in Figure 3.4 (f_F = 8.35Hz) but with a cut-off frequency of 100 Hz instead of 10 Hz. In this analysis the highest value of the bending moment, which is shown in Figure 3.7 (a), is slightly higher than when a lower cut-off frequency was used. A study of the frequency response spectra illustrated in Figure 3.7 (b) reveals why. When a higher cut-off frequency is used the excitation of mode number 5 (f = 74.71 Hz) is included in the analysis.

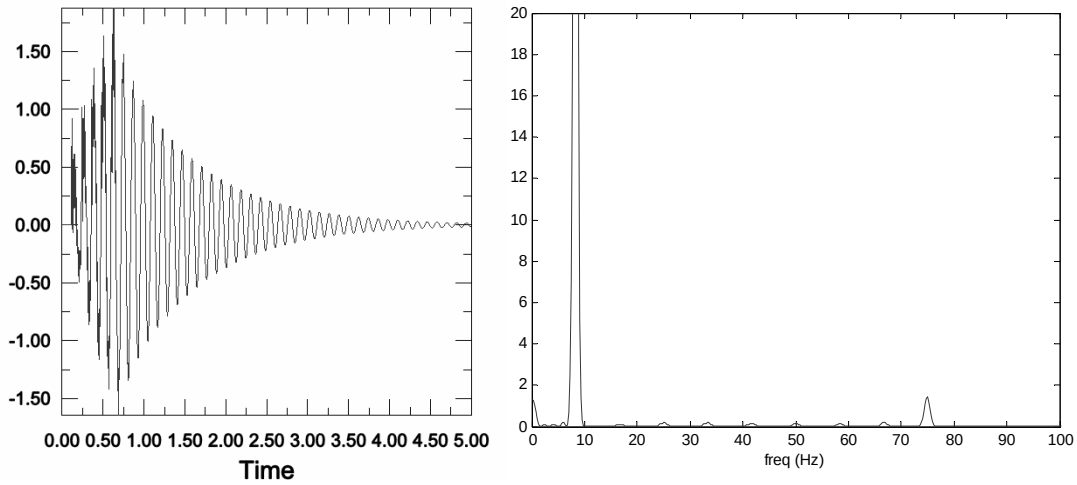

***Figure 3.7**: **(a)** Time history for the bending moment (SM1) at the centre of the beam when force F was applied 5 times with a frequency of 8.35Hz. Cut-off frequency 100Hz. **(b)** The bending moment time history transformed into the frequency plane through FFT.*

Nonetheless, not as many modes as the model's degree of freedom need to be included since, according to the reasoning mentioned previously, higher modes will have time to damp out before the force is reapplied. This is indicated in Figure 3.7 (b) where the amplitude of the exited mode at 74.71 Hz is not as high as the low frequency mode at 8.35 Hz is. Moreover, the precise correlation between the amplitudes at different frequencies in the frequency spectra, as well as the relation between the belonging mode's effects on the structure, is not fully established.

Therefore, the aim is to find a multiple of the highest frequency that the high-speed trains generate, and subsequently choose that frequency as the cut-off frequency in the modal analysis of the bridges. Modes with a higher frequency than the chosen cut-off frequency are considered to not critically affect the bridge.

3.3 Train load frequencies

The various frequencies the HSLM trains generate depend on the geometry and speed of the train and can be calculated analytically with Equation 2.7. Internal axle distance and resulting frequencies corresponding to a speed of 300 km/h are presented below in Table 3.1. The internal axle distances A-E referred to in Table 3.1 are explained in Figure 3.8. Notice that the highest frequency 41.7 Hz is generated when the distance A is 2 meters.

Vehicle		A	B	C	D	E
HSLM-A1	L [m]	2	3	11	16	18
	f [Hz]	41.7	27.8	7.6	5.2	4.6
HSLM-A2	L [m]	3.5	3	11	15.5	19
	f [Hz]	23.8	27.8	7.6	5.4	4.4
HSLM-A3	L [m]	2	3	11	18	20
	f [Hz]	41.6	27.8	7.6	4.6	4.2
HSLM-A4	L [m]	3	3	11	18	21
	f [Hz]	27.8	27.8	7.6	4.6	4
HSLM-A5	L [m]	2	3	11	20	22
	f [Hz]	41.6	27.8	7.6	4.2	3.8
HSLM-A6	L [m]	2	3	11	21	23
	f [Hz]	41.6	27.8	7.6	4	3.6
HSLM-A7	L [m]	2	3	11	22	24
	f [Hz]	41.6	27.8	7.6	3.8	3.5
HSLM-A8	L [m]	2.5	3	11	22.5	25
	f [Hz]	33.3	27.8	7.6	3.7	3.3
HSLM-A9	L [m]	2	3	11	24	26
	f [Hz]	41.6	27.8	7.6	3.5	3.2
HSLM-A10	L [m]	2	3	11	25	27
	f [Hz]	41.6	27.8	7.6	3.3	3.1

Table 3.1: *Different frequencies generated by different vehicles (trains) when travelling at 300 km/h*

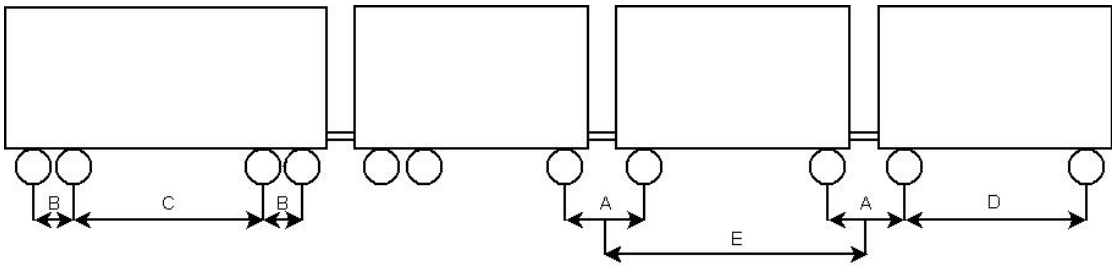

Figure 3.8: *The significant internal distance of the train.*

4 Standards and recommendations for analysis

4.1 Loads

According to the Swedish design code for railway bridges BV BRO [2], bridges trafficked by high-speed trains should be dynamically analysed with loads HSLM-A or HSLM-B. Load HSLM-A should be used for all bridges except for simply supported one-span bridges less than 7.0 meters where HSLM-B should be used. Bridges in which HSLM-B can be used will not be considered in this report.

HSLM-A simulates actual trains and consists of 10 different vehicles that should be checked for every single bridge. The load distribution and the load cases are shown in Figure 2.2 and Table 4.1.

Load case	Number of inter-mediate wagons [N]	Length of wagon D [m]	Bogie distance d [m]	Axis load P [kN]
HSLM-A1	18	18	2.0	170
HSLM-A2	17	19	3.5	200
HSLM-A3	16	20	2.0	180
HSLM-A4	15	21	3.0	190
HSLM-A5	14	22	2.0	170
HSLM-A6	13	23	2.0	180
HSLM-A7	13	24	2.0	190
HSLM-A8	12	25	2.5	190
HSLM-A9	11	26	2.0	210
HSLM-A10	11	27	2.0	210

***Table 4.1**: Train definitions according to [2]*

Each vehicle should, for every bridge, be tested in a velocity interval from 100 km/h to $1.2 \cdot v_{max}$ (i.e. 300 km/h). In the velocity interval, the velocity step can be increased with a maximum of 5 km/h between each velocity controlled.

4.2 Damping

The maximum structural damping values in the bridge, which can be used in the dynamic analysis, are shown in Table 4.2. The damping depends on the bridge type and span length. The damping ratio is the same for all modes in an analysis.

Type of bridge	ζ upper limit for damping (%)	
	L < 20 m	L ≥ 20 m
Steel- and composite constructions	ζ = 0.5+0.125(20-L)	ζ = 0.5
Prestressed concrete constructions	ζ = 1.0+0.07(20-L)	ζ = 1.0
Reinforced concrete constructions	ζ = 1.5+0.07(20-L)	ζ = 1.5

***Table 4.2**: Bridge damping according to [2]*

4.3 Boundary conditions

The knowledge about the deformation properties of soil materials in fast dynamic events is inadequate. The stiffness is significant larger than the well-known stiffness that soil has when being subjected to a permanent load. Since the Swedish design code for railway bridges BV BRO [2] does not demand that the deformation of the soil has to be considered, it is most common to model the soil as rigid in bridge designing, because the possibilities of meeting the demands of vertical acceleration increase.

4.4 Practical recommendations

4.4.1 Time increment

During a modal dynamic analysis, a fixed time increment (Δt) is used. The user must specify this time increment. When designing structures there should be at least 10 time increments per period (T) of the highest frequency (f_{max}) of the analysis (i.e. the cut-off frequency) in order to receive accurate results.

$$\Delta t \leq \frac{T_{\min}}{10} = \frac{1}{10 f_{\max}} \tag{4.1}$$

For example, if an analysis with a cut-off frequency of 50 Hz is to be performed, the time increment (Δt) should be chosen as 0.002 (=1/500) seconds or lower.

4.4.2 Convergence criteria

To determine at which level the analyses converge, reference cut-off frequencies for both bridge 1 and bridge 2 is chosen so high that the results from those analyses are considered to be satisfying. The reference cut-off frequencies for these analyses are 70 Hz and 180 Hz for bridge 1 and bridge 2 respectively. For bridge 1, the reference cut-off frequency was chosen through experience from earlier analyses made on a similar bridge. For bridge 2, the reference cut-off frequency was chosen based on the assumption used in other structure designing fields, that a cut-off frequency higher than four times the highest load frequency should not be necessary. If the results from

an analysis differ less than 10 % from the analysis with reference cut-off frequency, the results assumed to have converged.

The requirement of a difference less than 10 % does not necessarily concern all points along the bridges. When studying the convergence of shear forces, only areas near the supports, where the force will peak, are of interest. Also, only the magnitude of the greatest maximum or minimum value in these areas is of interest when designing a bridge. The sign of the value is not important. When designing the bridge regarding the bending moment, both the maximum and minimum bending moments are relevant to study since they are used to design the lower and upper reinforcement, respectively. However, in areas where the bending moment is relative small, the percentage increase does not matter since the difference in value is rather small.

5 Modelling

5.1 General modelling of bridges

5.1.1 Element types

For the modelling of superstructures, end shields and wing walls general-purpose four node shell elements with reduced integration and a large-strain formulation are used. This type of general-purpose element provides accurate solution in all loading conditions for both thin and thick shell problems. For the modelling of the edge beams and columns, Timoshenko beams are used. Timoshenko beams are described by two node elements and allow transverse shear deformation and can be used for thick as well as slender beams [4].

5.1.2 Boundary conditions

In agreement with common practice, the ground is not modelled as deformable in the bridge models. Instead all supports have been fixed in all degrees of freedom at foundation level. [2]

5.1.3 Residual modes

The residual mode shape and frequency are calculated in the frequency step of the analysis. The use of residual modes requires that a static load case is added to the structure in a linear perturbation step prior the frequency step. This load case is used to calculate the mode shape and frequency. Recommendations suggest that this staic load case is defined as similar to the dynamic load as possible [4]. Since the dynamic load i.e. the trainload, is moving along the rail as point loads there is no absolute way to design the load case. To investigate how the load case should be designed to get the best result, two different load case shapes have been tested. In the first case, the load was applied as point loads along the rails. A distributed load was applied on the entire deck of the bridge in the second case. These two alternatives were carried out for both bridges.

5.1.4 Modelling of trains

The trainloads are according to standard defined as N numbers of point loads moving in pairs that are spaced with different distances for each train model [2]. In BRIGADE/Plus, the different HSLM trainloads are predefined and applied as external forces along the rails with a load intensity history simulating axles approaching and leaving.

5.1.5 Material properties

In order to include the weight of the ballast (the bed of stones fixating the rails) on the deck, fictitious densities have been introduced in different areas. The fictional densities are calculated as shown in Equation. 5.1.

$$\rho_{fictional} = \rho_{concrete} + \rho_{ballast} \cdot H_{ballast} / H_{concrete} \quad (5.1)$$

were $H_{ballast}$ is the average ballast thickness and $H_{concrete}$ is the bridge thickness in the area of interest.

In accordance with common practice the structural stiffness used in models correspond to the stiffness of uncracked concrete. Since the reinforcement is of interest for cracked concrete only, it is not included in this model.

5.2 Bridge 1

5.2.1 Geometry

Bridge 1, shown in Figure 5.1, is a three span reinforced concrete bridge. The length of the bridge is 41.5 meter and the width is 7 meter. The mid span and end spans measures 15 and 12 meter respectively. The deck thickness is 0.95 meter. At the distance of 6.4 meter from each of the mid supports the thickness start increasing with a parabolic shape to be 1.5 meter at the support line. The end shields and wing walls are 0.7 meter thick respectively. The columns are 8.5 meters high, measured from the bridge's centre of gravity and have circular cross sections with a diameter of 1.2 meter. Every pair of columns is spaced with 3 meters, which is measured between their centrelines. The two edge beams used to keep the ballast in place, one beam on each long side of the bridge, have a rectangular profile with a width of 0.6 meter and a height of 0.8 meter.

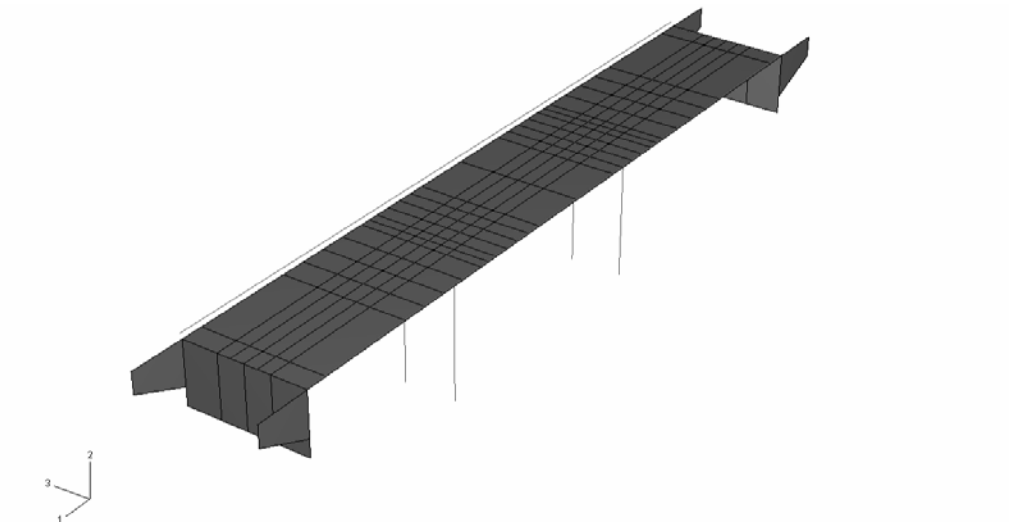

***Figure 5.1**: Geometric model of bridge 1*

5.2.2 Material property

The bridge is made of concrete with Young's modulus E = $34 \cdot 10^9$ N/m^2 and Poisson's ratio ν = 0.2. With a concrete density of 2500 kg/m^3, a ballast density of 2000 kg/m^3 and an average ballast thickness of 450 millimetres Equation 5.1 become:

$$\rho_{fictional} = 2500 + 2000 \cdot 0.45 / H_{concrete} \tag{5.2}$$

The fictitious density in different sections of the deck, as well as the thickness of each section, is presented in Table 5.1 and Figure 5.2.

Section	Bridge thickness [m]	Fictitious Density [kg/m^3]
1	0.950	3447
2	0.959	3438
3	1.027	3376
4	1.165	3273
5	1.371	3156
6	1.500	3100

Table 5.1: *Density in different sections of the deck.*

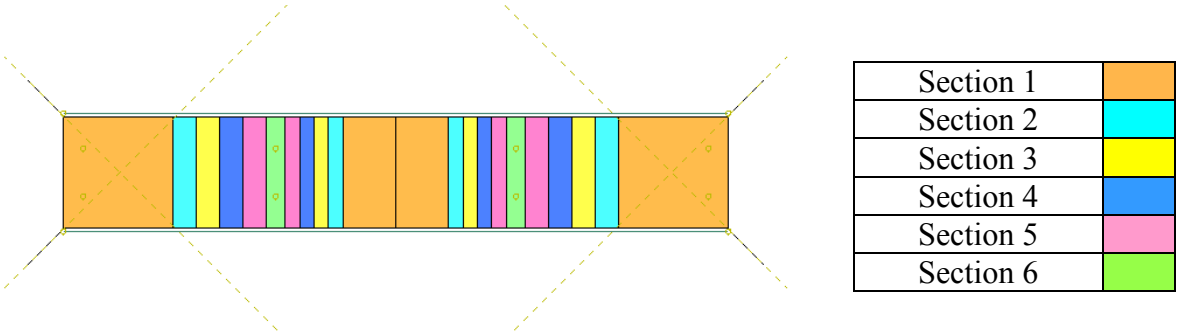

Figure 5.2: *The sections of the deck. View form above.*

The damping ratio ζ for bridge 1 is set to 1.5 % in agreement with BV BRO [2].

5.2.3 Interaction and boundary conditions

The edge beams interact with the deck using rigid beam connection.

As mentioned in 5.1.2 the ground is modelled as un-deformable. The lower edges of the columns are therefore fixed in all degrees of freedom. The end supports have not been modelled. Instead, at the end supports, the nodes above each bearing point are locked for vertical translation and translation in the bridge's cross-direction but free to move in all other directions.

5.2.4 Dynamic loads

Vehicles HSLM-A1, HSLM-A3 and HSLM-A4 have been analysed in velocities between 100 and 300 km/h. The vehicles have been loaded along the two node lines shown in Figure 5.3. The lines are respectively distanced 0.75 meter from the centre-line.

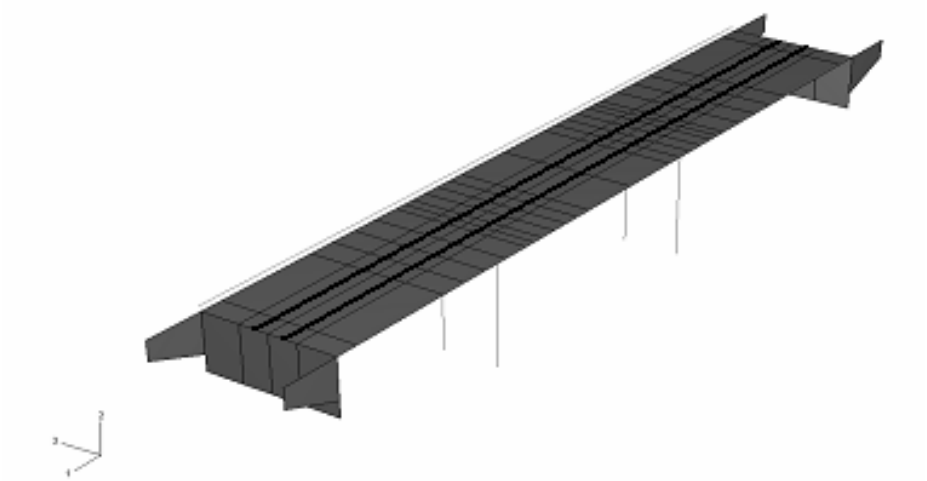

Figure 5.3: *Rail positions where trainloads have been applied.*

For the dynamic load, a small output area along one rail is defined. It is advantageous to use as small output field as possible to save computational time and minimize the size of the result files. The most critical areas of the bridge are near the rails, especially near the midfield of the spans and the areas near the supports. Since the bridge is symmetric, the output area only contains one of the rails. The output area starts at one of the end shields and ends at the centre of the mid span.

5.2.5 Mesh

As mentioned in 5.1.1, four node elements have been used to mesh the deck, the end shield and the wing walls and two node elements to mesh the edge beams and columns. The elements sizes of the deck are approximately 0.7 x 0.7 meter. Figure 5.4 shows the mesh of bridge 1.

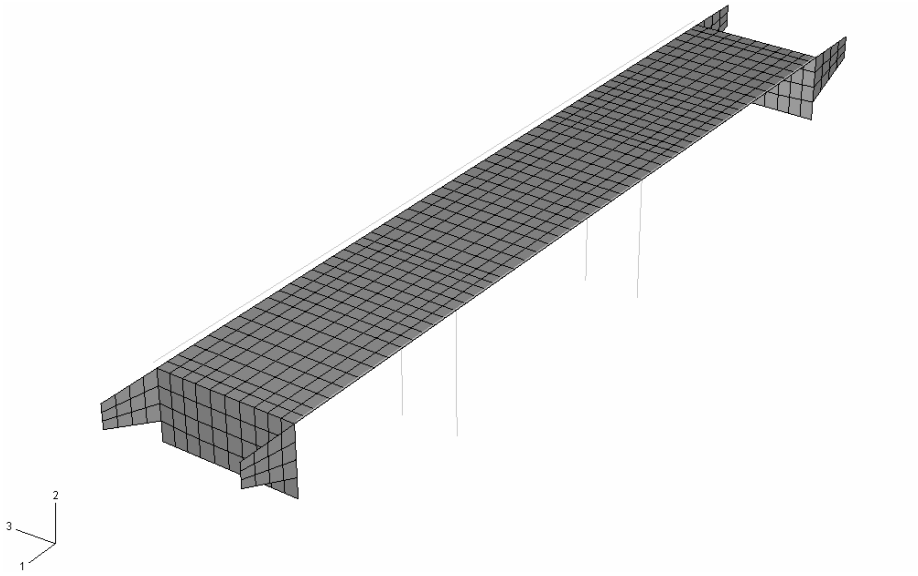

***Figure 5.4**: Mesh of Bridge 1*

5.2.6 Analysis

There are 5 cut-off frequencies tested for each vehicle on bridge 1. The dynamic analyses have been performed with modal superposition and are based on eigenmodes up to 30, 40, 50, 60 and 70 Hz. The time increment for each analysis has been chosen as described in chapter 3.4 and the output data is saved for each time increment.

5.3 Bridge 2

5.3.1 Geometry

Bridge 2 is chosen because short frame bridges have relatively high eigenfrequencies and therefore gives a good indication of an upper limit of cut-off frequency. Bridge 2 is a frame bridge with two rail tracks and is used for crossing a pedestrian path. The bridge's frame consists of a 3.5 meter span, an 11.2 meter width and a height of 3.75 meter. The four wing walls are 4.8 meter long and their height varies between 4.90 and 1.30 meter. The bridge also consists of two edge beams that are connected to the deck. A shell model is used for all parts of the bridge except for the edge beams. Bridge 2 is shown in Figure 5.5.

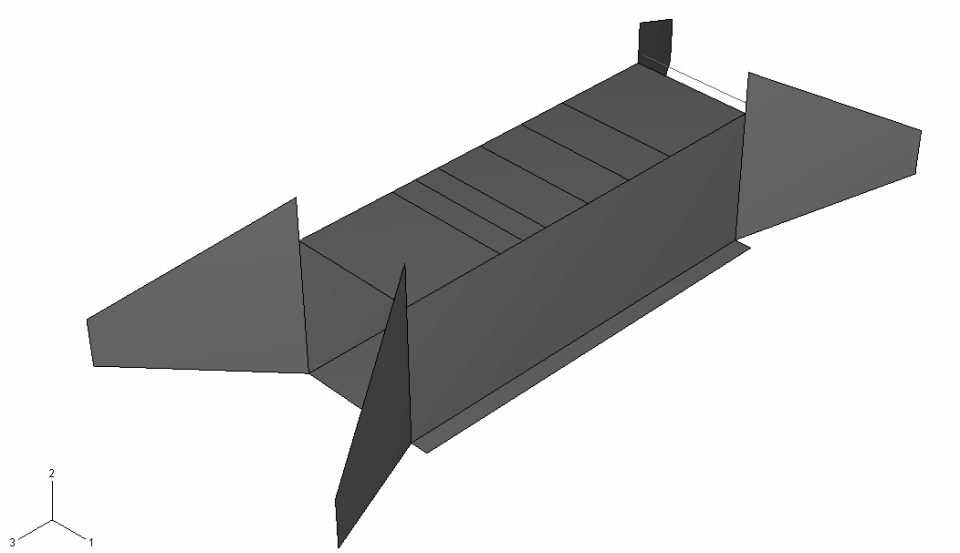

***Figure 5.5**: Geometric model of bridge 2*

5.3.2 Material property

The bridge is made of concrete with Young's modulus $E = 34 \cdot 10^9$ N/m^2 and Poisson's ratio $\nu = 0.2$. As mentioned in 5.1.5, the density of the deck is modified to make up for the weight of the ballast. The thickness of the bridge is not the same in all sections and is therefore shown in table 5.2, together with the density of the sections.

Section	**Bridge thickness [m]**	**Density [kg/m^3]**
Deck	0.5	4900
Abutment	0.5	2500
Foundation slab	0.6	2500
Wings	0.4	2500

***Table 5.2**: Density of different section of bridge 2.*

The edge beams have a rectangular profile with a width of 0.25 m and a height of 0.8 m.

5.3.3 Interaction and boundary conditions

The edge beams interact with the deck using rigid beam connection in order to get a desirable interaction. As noted, the foundation slab is fixed in all directions according to 5.1.2.

5.3.4 Dynamic loads

Vehicles HSLM-A1 and HSLM-A10 are analyses of velocities from 100 km/h to 300 km/h. A1 is analysed because it has the shortest distance between the point loads and A10 is analysed because it has the largest load magnitude.

An output area for the dynamic loads on bridge 2 was defined along one of the rails. To keep the output data file as small as possible, the output area contains only one row of element along one of the rails. The rails for bridge 2 are shown in Figure 5.6.

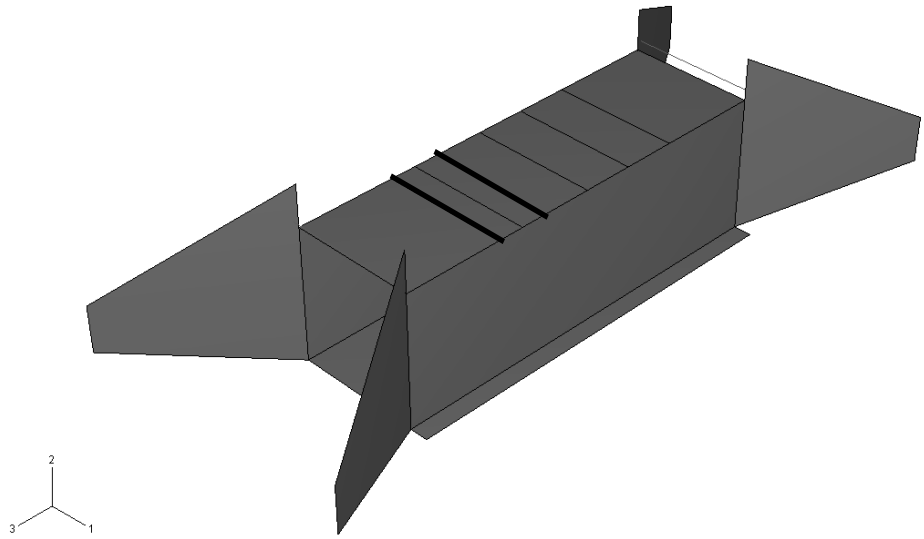

Figure 5.6: *Rail positions where trainloads have been applied.*

5.3.5 Mesh

Four node elements have been used to mesh the structure, see section 5.1.1. Since the largest result gradient will occur on the deck, this area has a finer mesh than the rest of the structure. The elements sizes on the deck are approximately 0.3 x 0.7 meter. Since the foundation slab is fixed and thus will not deform at all, it consists of a course mesh. Figure 5.7 shows the mesh of bridge 2.

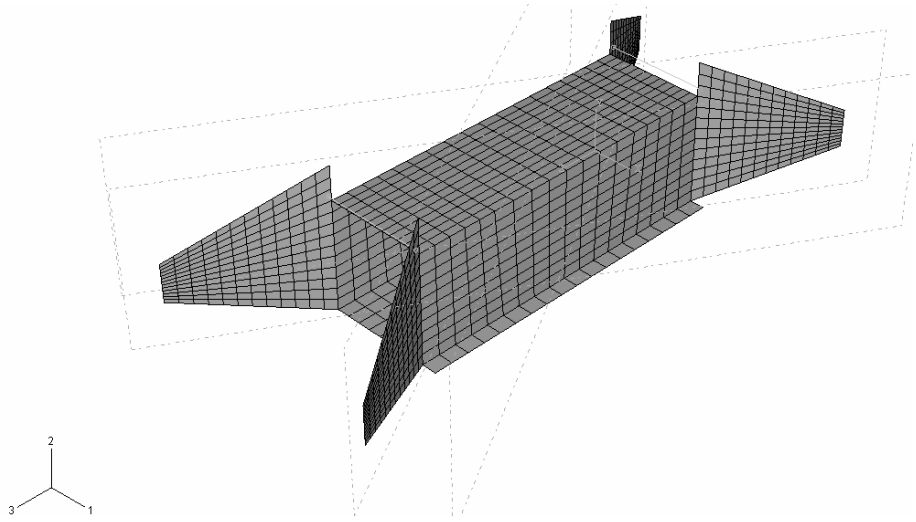

***Figure 5.7**: Mesh of Bridge 2*

5.3.6 Analysis

There are 9 cut-off frequencies tested for the two vehicles on bridge 2. The dynamic analyses have been performed with modal superposition and are based on eigenmodes up to 80, 100, 120, 140, 150, 160 and 180 Hz respectively. The time increment for each analysis has been chosen as described in chapter 3.4. Output data is saved for every time increment.

6 Results of dynamic analyses

6.1 Eigenfrequencies

6.1.1 Bridge 1

Bridge 1 has 44 eigenmodes below 70 Hz, see Table 6.1. Appendix A shows the shape of the most important modes.

Eigenmode	Frequency [Hz]	Description	Eigenmode	Frequency [Hz]	Description
1	2.11	Horizontal translation	23	40.46	End shields/wing walls
2	6.95	Horizontal bend mode	24	43.38	End shields/wing walls
3	8.55	Vertical bend mode	25	44.38	End shields/wing walls
4	11.20	Vertical bend mode	26	45.53	End shields/wing walls
5	13.79	Vertical bend mode	27	45.78	Columns
6	16.32	Torsional mode	28	46.77	Columns
7	20.62	Torsional mode	29	46.77	Columns
8	20.86	Vertical bend mode	30	47.11	Columns
9	20.99	Vertical bend mode	31	47.77	Columns
10	22.18	Wing walls	32	48.01	Columns
11	24.14	Wing walls	33	48.47	Columns
12	24.82	Wing walls	34	49.90	Columns
13	25.08	Wing walls	35	51.84	Columns
14	25.08	Wing walls	36	54.84	End shields
15	25.48	Wing walls	37	55.87	Torsional mode
16	26.34	Wing walls	38	56.13	End shields
17	26.40	Wing walls	39	63.52	End shields/wing walls
18	26.47	Vertical bend mode	40	63.54	End shields/wing walls
19	34.40	Torsional mode	41	65.34	Vertical bend mode
20	35.61	Vertical bend mode	42	65.84	Vertical bend mode
21	37.95	Wing walls	43	67.11	Vertical bend mode
22	39.13	Vertical bend mode	44	68.29	Horizontal bend mode

***Table 6.1**: Eigenfrequencies for Bridge 1*

6.1.2 Bridge 2

Table 6.2 shows the 54 eigenfrequencies below 180 Hz. The description of the modes can be seen in Table 6.2 while the most important mode shapes are shown in Appendix B. Note that the higher modes are complex and therefore difficult to describe appropriately.

Eigenmode	Frequency [Hz]	Description	Eigenmode	Frequency [Hz]	Description
1	11.40	Wing walls	28	112.18	Wing walls
2	11.75	Wing walls	29	113.02	Vertical bend mode
3	11.96	Wing walls	30	114.85	Horizontal bend mode
4	11.96	Wing walls	31	116.72	Wing walls
5	14.94	Horizontal translation	32	116.74	Wing walls
6	31.92	Torsional mode	33	118.55	Horizontal bend mode
7	47.87	Wing walls	34	119.02	Wing walls
8	49.13	Wing walls	35	125.65	*Complex*
9	49.24	Wing walls	36	129.10	*Complex*
10	52.68	Wing walls	37	129.40	*Complex*
11	53.81	Wing walls	38	137.52	*Complex*
12	57.47	Wing walls	39	142.89	*Complex*
13	57.79	Wing walls	40	144.16	*Complex*
14	58.02	Wing walls	41	145.45	*Complex*
15	59.86	Wing walls	42	148.04	*Complex*
16	61.97	Vertical bend mode	43	155.01	*Complex*
17	66.47	Vertical bend mode	44	155.60	*Complex*
18	70.39	Vertical bend mode	45	156.42	*Complex*
19	72.41	Wing walls	46	157.62	*Complex*
20	73.71	Wing walls	47	159.81	*Complex*
21	81.05	Vertical bend mode	48	161.45	*Complex*
22	82.58	Horizontal bend mode	49	166.48	*Complex*
23	92.57	Wing walls	50	167.32	*Complex*
24	95.12	Vertical bend mode	51	169.21	*Complex*
25	103.11	Wing walls	52	178.22	*Complex*
26	106.32	Wing walls	53	179.70	*Complex*
27	106.79	Vertical bend mode	54	179.92	*Complex*

***Table 6.2**: Eigenfrequencies for Bridge 2*

6.2 Residual modes

The two different designed load cases tested for bridge 1, results in different shaped residual modes. The residual modes resemble the solutions of the static perturbation step, which is to expect according to [4]. The solution of the static perturbation step and the shapes of the residual modes for cut-off frequencies 30, 40, 50 and 60 Hz are shown in Figure 6.1 and 6.2.

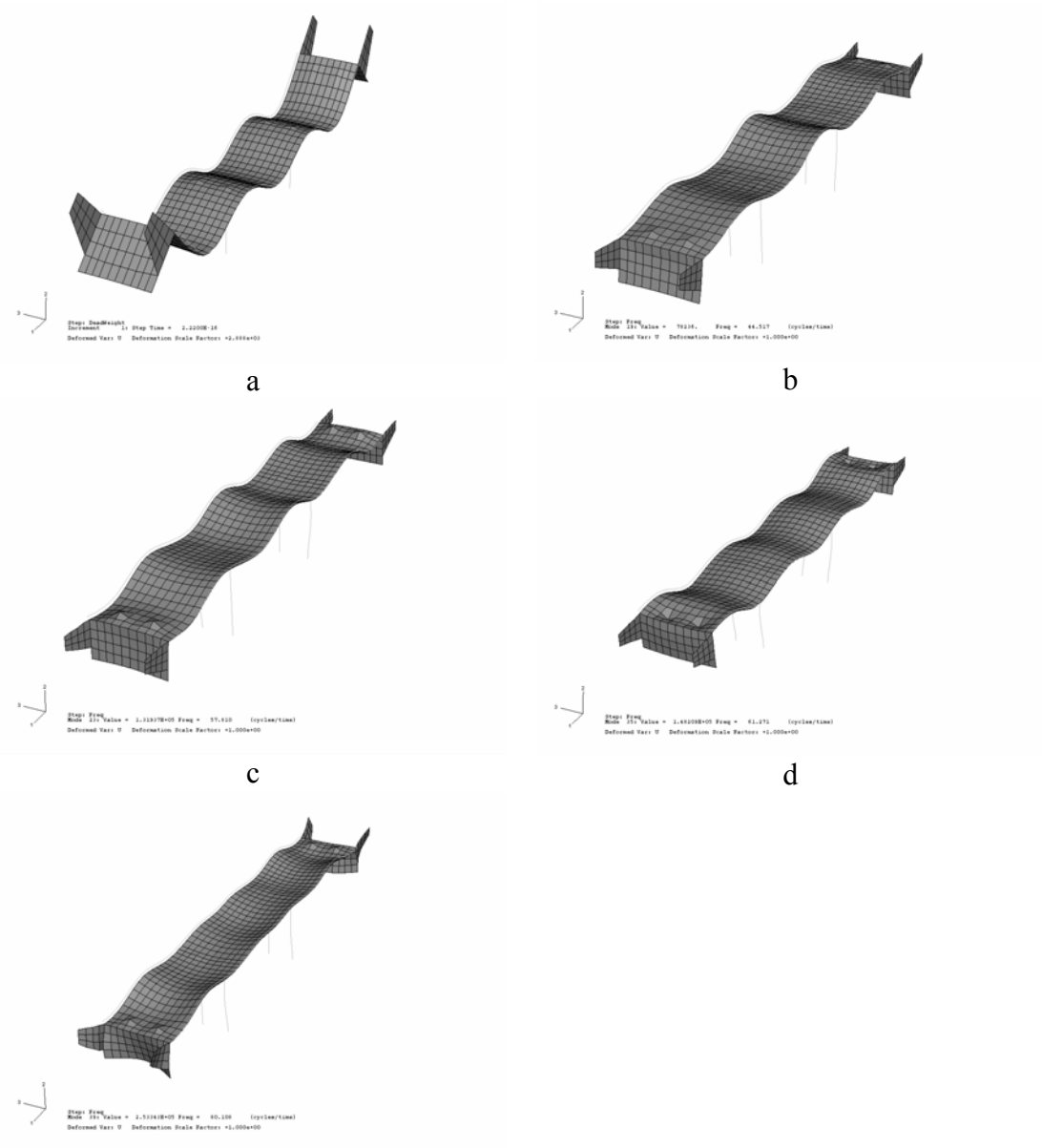

a b c d e

***Figure 6.1**: **(a)** Solution of the static perturbation step with distributed load on the deck. Shape of residual mode for analysis with cut-off frequency **(b)** 30 Hz, **(c)** 40 Hz, **(d)** 50 Hz and **(e)** 60 Hz.*

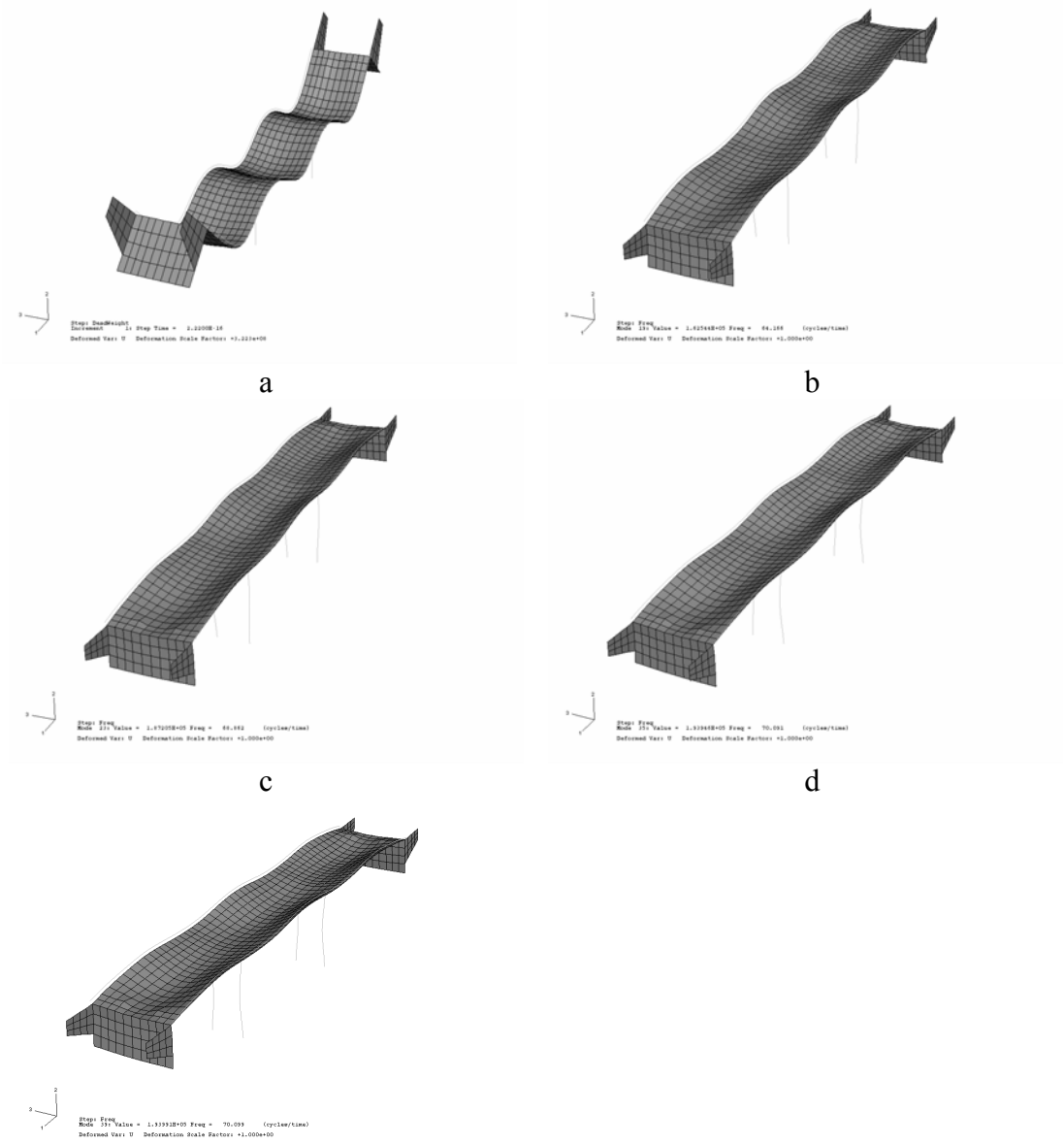

a b c d e

***Figure 6.2**: **(a)** Solution of the static perturbation step with the load applied as concentrated forces along the rails. Shape of residual mode for analysis with cut-off frequency **(b)** 30 Hz, **(c)** 40 Hz, **(d)** 50 Hz and **(e)** 60 Hz.*

The solution of the static perturbation step and the shapes of the residual modes for bridge 2 when applying the two different load cases, using cut-off frequencies 80, 100 and 120 Hz are shown below in Figure 6.3 and 6.4.

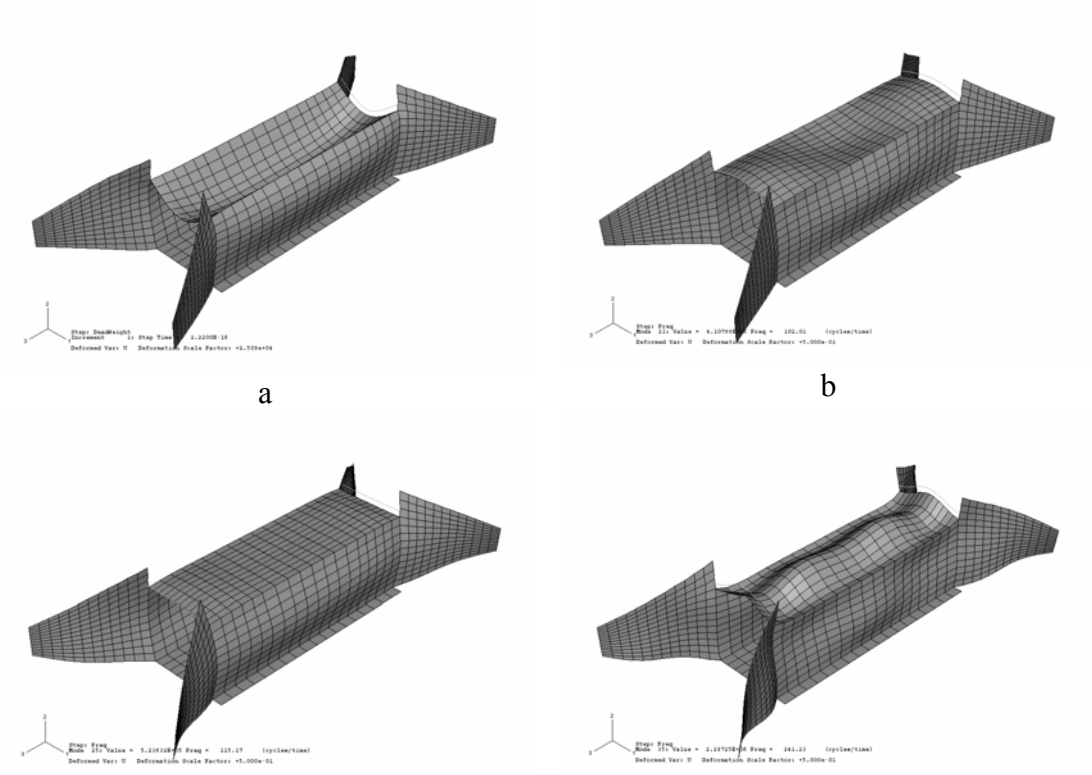

a b

c d

***Figure 6.3**: **(a)** Solution of the static perturbation step with distributed load on the deck. Shape of residual mode for analysis with cut-off frequency **(b)** 80 Hz, **(c)** 100 Hz and **(d)** 120 Hz.*

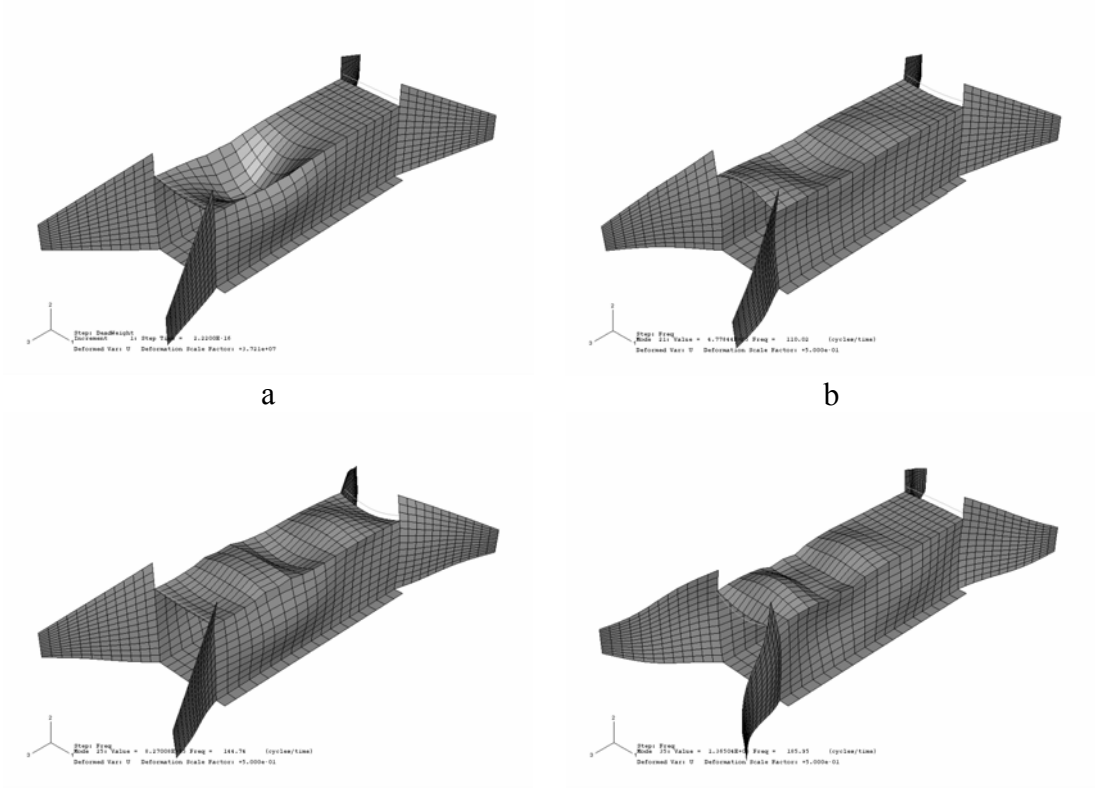

a b

c d

***Figure 6.4**: **(a)** Solution of the static perturbation step with the load applied along the rails. Shape of residual mode for analysis with cut-off frequency **(b)** 80 Hz, **(c)** 100 Hz and **(d)** 120 Hz.*

6.3 Cut-off frequencies without consideration to residual modes

6.3.1 Bridge 1

The maximum and minimum section force (shear force and bending moment) in each node, regardless from what speed and at what time the values arise from, were calculated using BRIGADE/Plus. These envelopes along a path, shown with a red arrow in Figure 6.5, are used to create a convergence plot for each dynamic load (vehicle). Since the section forces are of greatest interest in the centre of the spans and at the supports, the path is chosen to pass right above the bearing support and the column.

The plots for each vehicle are put together in a convergence plot to determine at what frequency the section forces converge. Figure 6.6-6.11 shows the convergence plots of the shear force and bending moment for the chosen dynamic loads mentioned in 5.2.4.

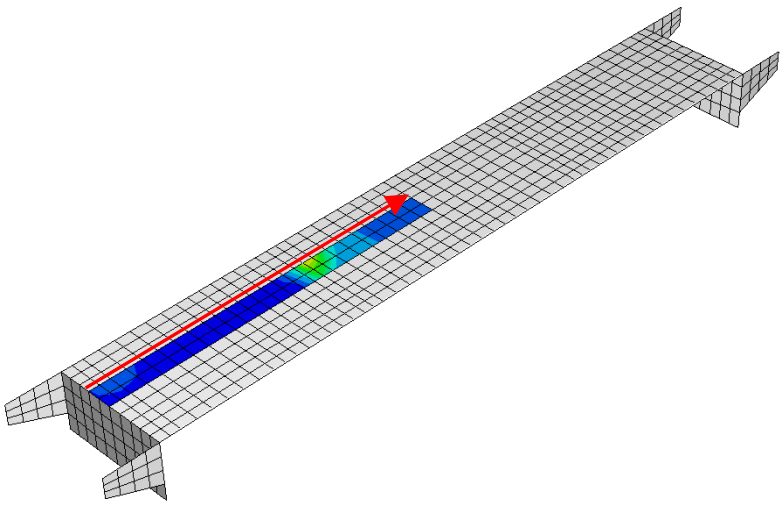

***Figure 6.5**: Created path for bridge 1*

HSLM-A1

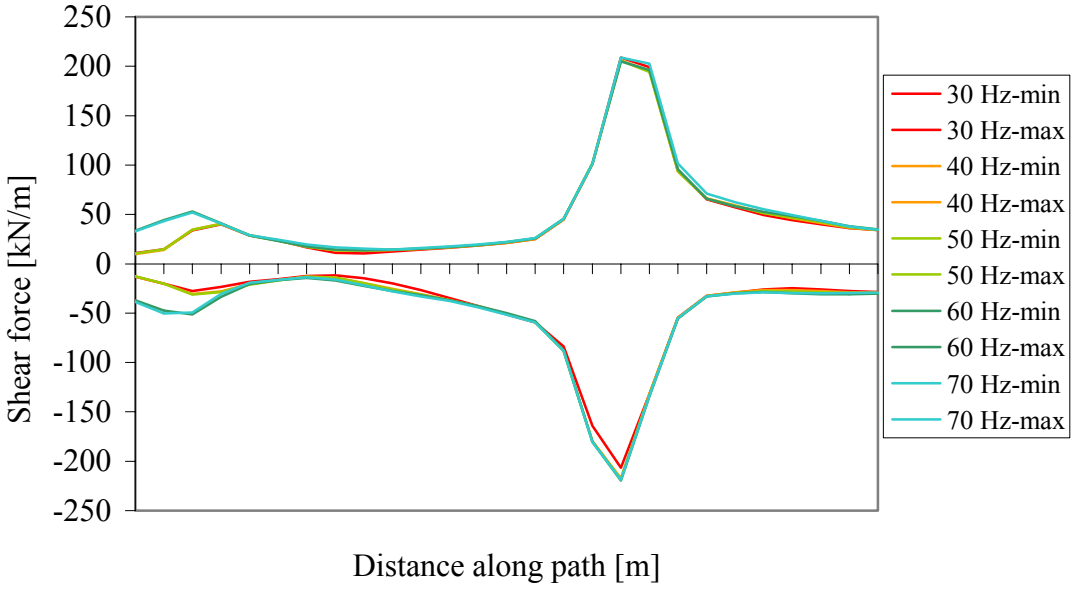

***Figure 6.6**: Maximum/minimum shear force from HSLM-A1 using different cut-off frequencies.*

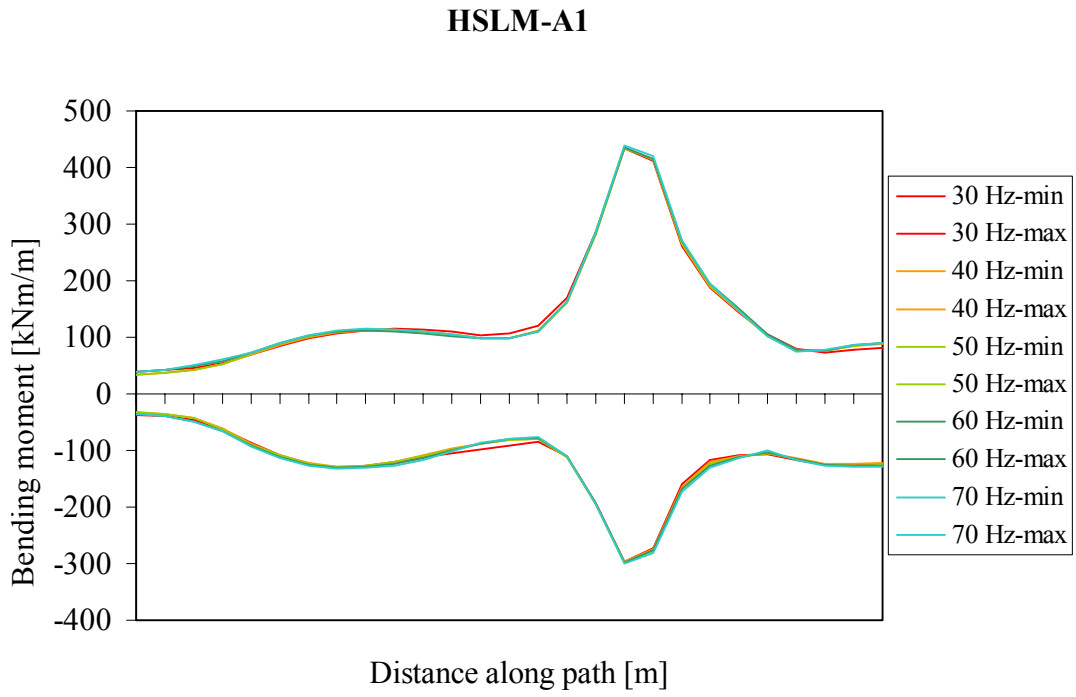

Figure 6.7: *Maximum/minimum bending moment from HSLM-A1 using different cut-off frequencies.*

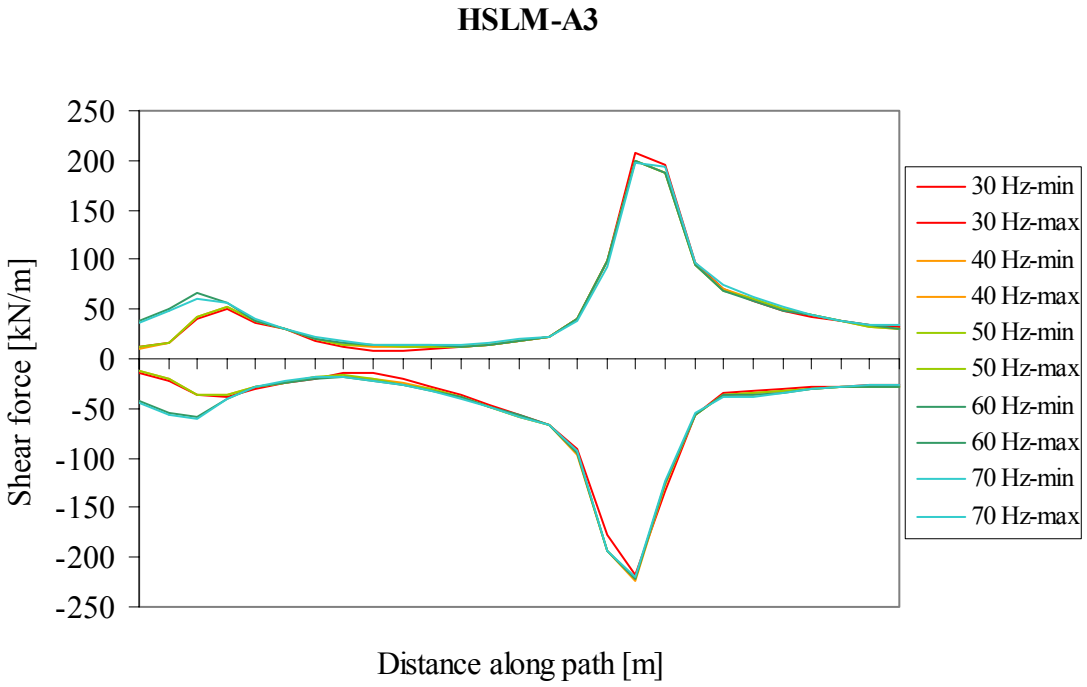

Figure 6.8: *Maximum/minimum shear force from HSLM-A3 using different cut-off frequencies.*

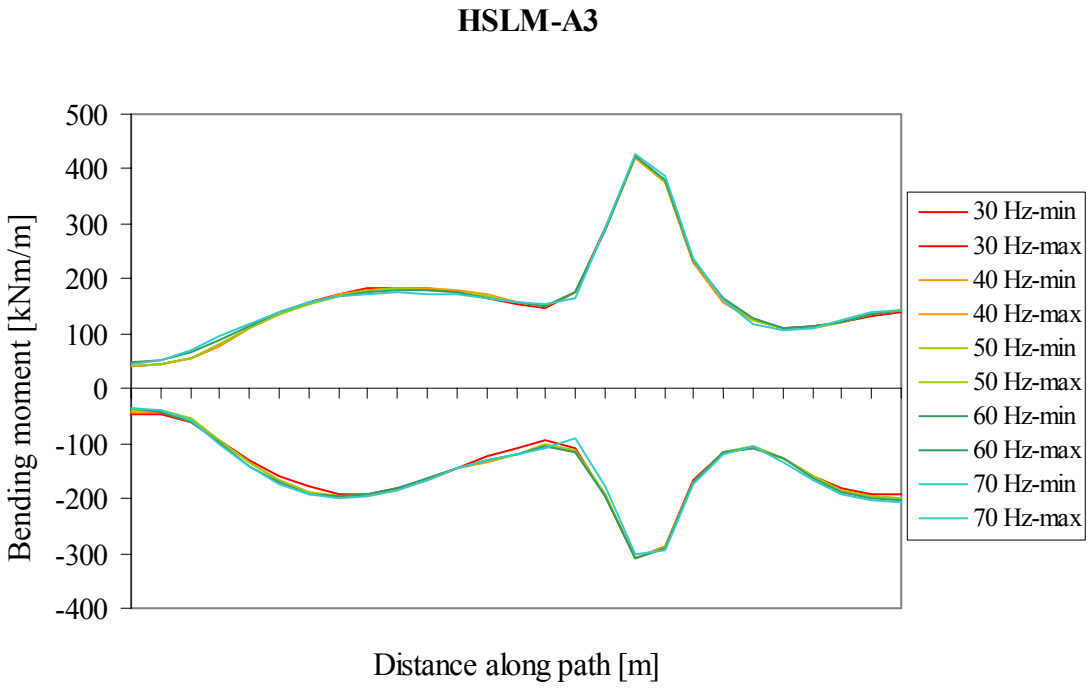

Figure 6.9: *Maximum/minimum bending moment from HSLM-A3 using different cut-off frequencies.*

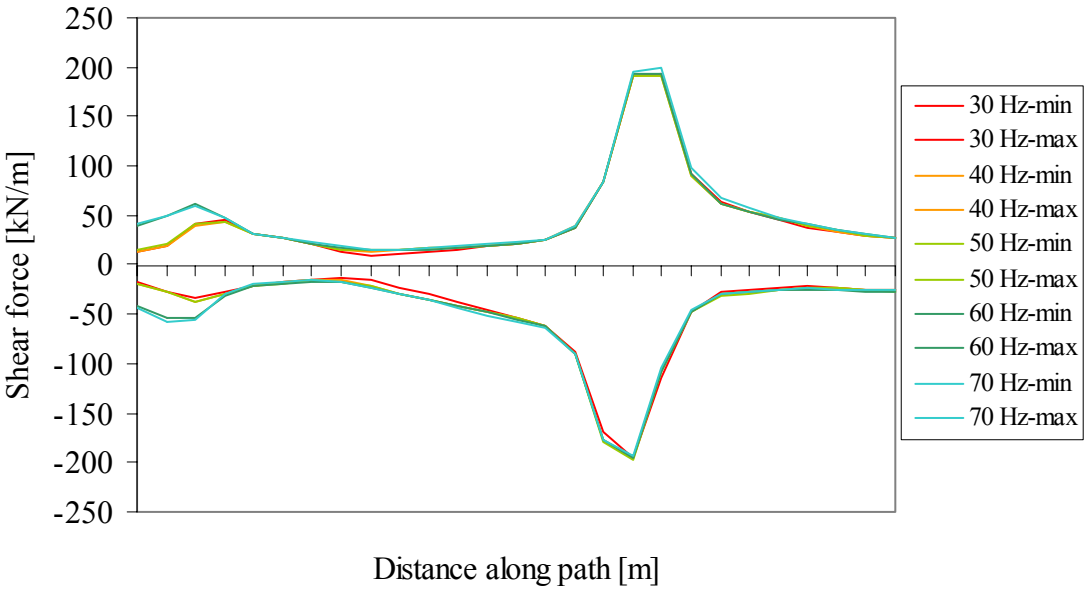

Figure 6.10: *Maximum/minimum bending moment from HSLM-A4 using different cut-off frequencies.*

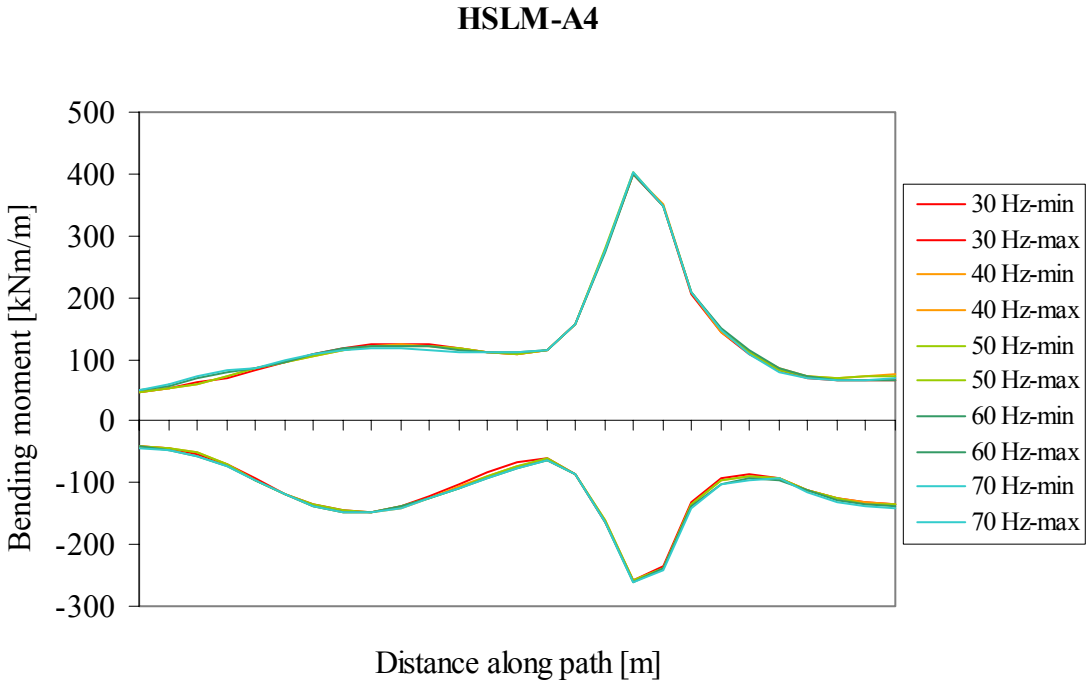

Figure 6.11: *Maximum/minimum shear force from HSLM-A4 using different cut-off frequencies.*

The convergence criterion is as mentioned in section 4.4.2 set to 10 %. The shear force has acceptable magnitudes in the critical areas when the cut-off frequency is 60 Hz while the bending moment converges earlier at the cut-off frequency 30 Hz.

6.3.2 Bridge 2

The maximum and minimum section forces are, as for bridge 1, calculated in BRIGADE/Plus. The section forces along one of the rails are analysed, from one abutment to the other. The path is shown with a red arrow in Figure 6.12. Along the path, two convergence plots for each dynamic load is created, one of shear force and one of bending moment. The plots are shown in Figure 6.13-6.16.

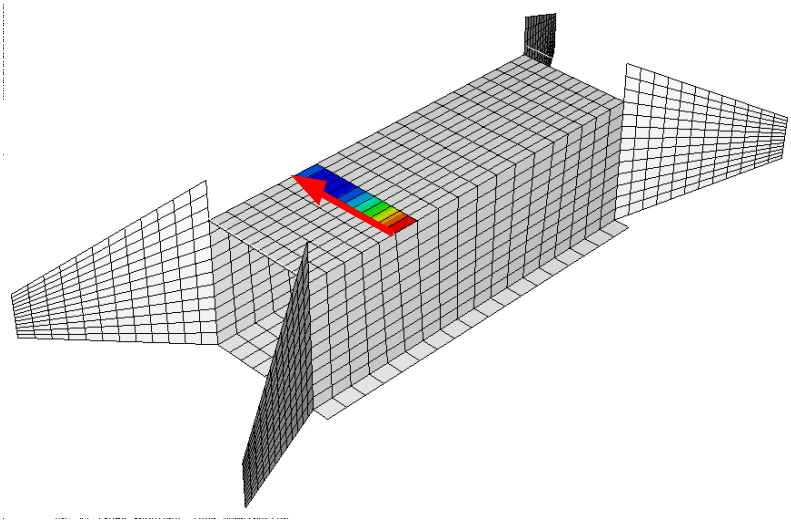

***Figure 6.12**: Path created for bridge 2.*

HSLM-A1

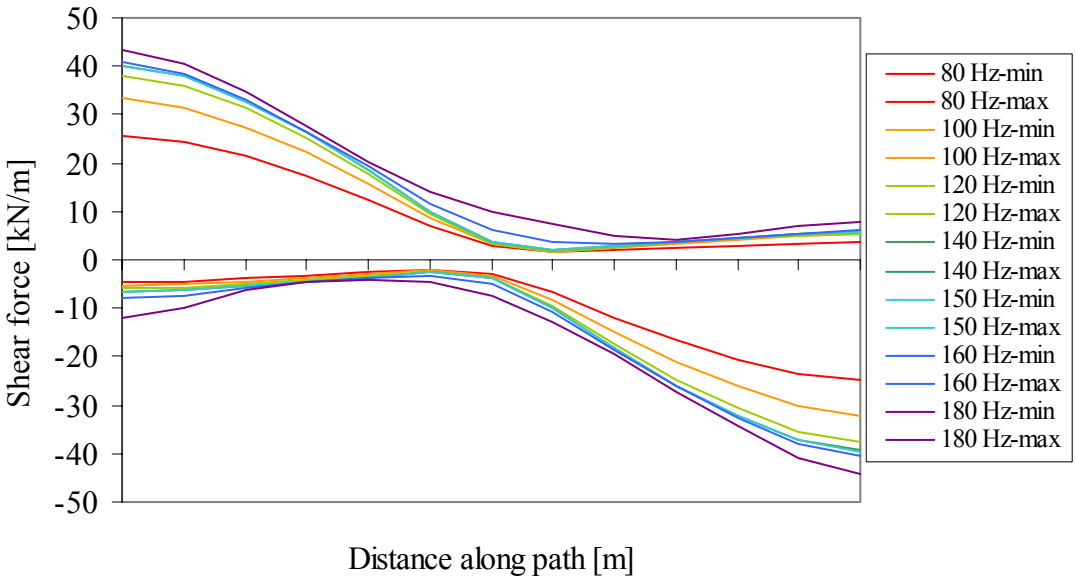

***Figure 6.13:** Maximum/minimum shear force from HSLM-A1 using different cut-off frequencies.*

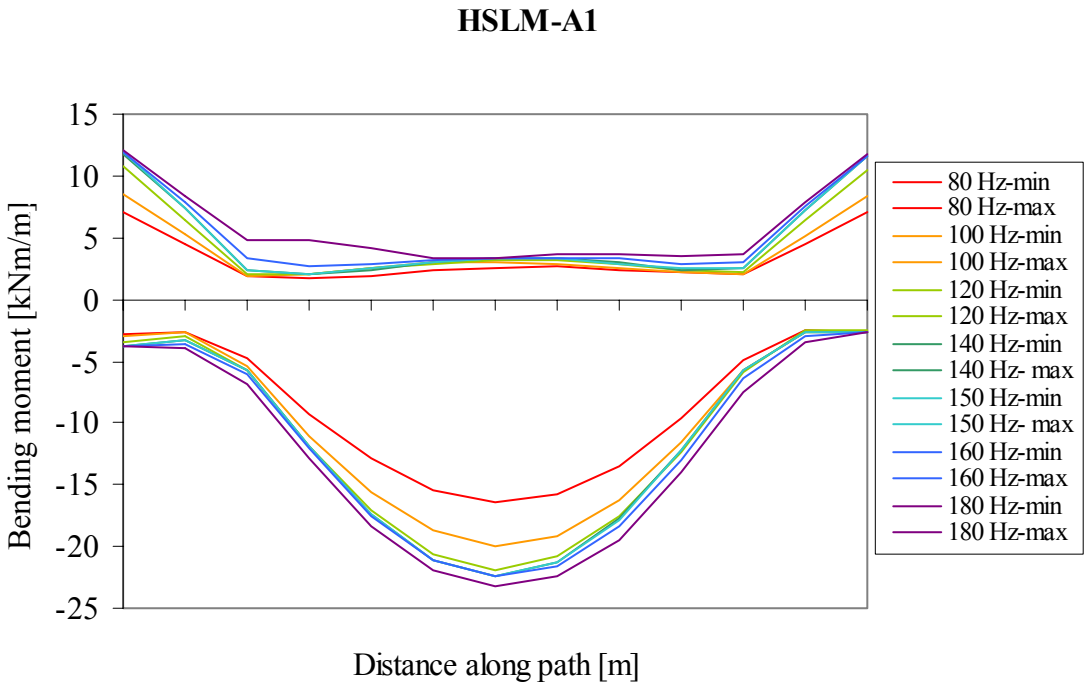

Figure 6.14: *Maximum/minimum bending moment from HSLM-A1 using different cut-off frequencies.*

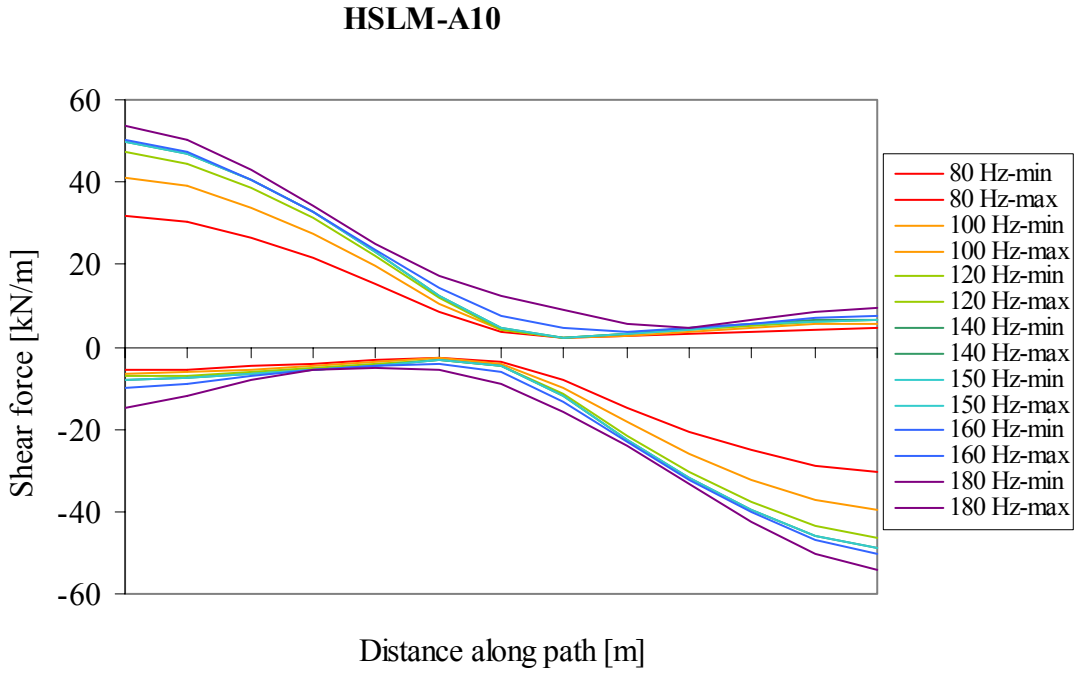

Figure 6.15: *Maximum/minimum shear force from HSLM-A10 using different cut-off frequencies.*

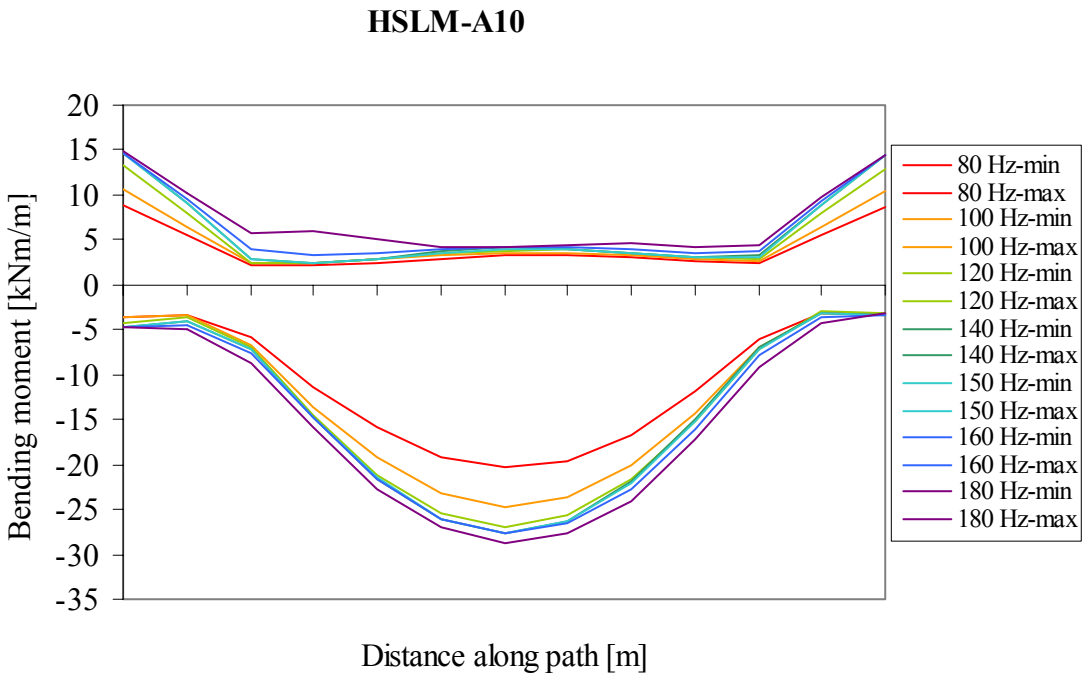

Figure 6.16: *Maximum/minimum bending moment from HSLM-A10 using different cut-off frequencies.*

Using the convergence criterion 10 %, both the shear force and the bending moments converge in all critical areas for the cut-off frequency 160 Hz.

The frequencies, at which the shear force and moment converge, and the chosen cut-off frequencies for the two bridges are presented in Table 6.3. For comparison with the effective mass method, the table also shows the percentage effective mass. The effective mass is here calculated as the ratio between sum of effective mass at the cut-off frequency (calculated in BRIGADE/Plus) and the total mass that is able move in the structure. The following conclusions can be made:

- The section forces converge at different cut-off frequencies for the two bridges when they are subjected to exactly the same load, in this case A1.
- For each bridge all tested vehicles converge at the same cut-off frequency.
- Shear force and bending moment converge at different cut-off frequencies in one of the studied bridges.

Bridge	Vehicle	Cut-off frequency regarding shear force [Hz]	Effective mass [%]	Cut-off frequency regarding bending moment [Hz]	Effective mass [%]	Chosen cut-off frequency [Hz]
1	A1	60	90	30	69	60
1	A3	60	90	30	69	60
1	A4	60	90	30	69	60
2	A1	160	56	160	56	160
2	A10	160	56	160	56	160

***Table 6.3**: Cut-off frequencies at which the analyses converge for bridge 1 and 2 together with the effective mass at the cut-off frequency.*

A comparison between the highest cut-off frequency needed to converge all studied section forces and the highest load frequency for each vehicle are analysed and presented in Table 6.4 and 7.3. It shows that, for bridge 1, the cut-off frequencies are never greater than 1.5 times the highest frequency that any vehicle can give rise to, see Table 6.4. For bridge 2, the cut-off frequencies never exceed 3.9 times the highest load frequency to which any of the vehicles can give rise to, see Table 6.5.

	A1	A3	A4
Highest load frequency	41.6	41.6	27.8
Cut-off frequency	60	60	60
Ratio	1.44	1.44	2.16

***Table 6.4**: A ratio between the cut-off frequency and the highest load frequency for bridge 1.*

	A1	A10
Highest load frequency	41.6	41.6
Cut-off frequency	160	160
Ratio	3.85	3.85

***Table 6.5**: A ratio between the cut-off frequency and the highest load frequency for bridge 2.*

6.4 Cut-off frequencies with consideration to residual modes

6.4.1 Bridge 1

Residual modes do not seem to have a great influence on the cut-off frequency for bridges like bridge 1. When including a residual mode in the analysis the shear force converges at the cut-off frequency 60 Hz, which is the same cut-off frequency discovered in the analyses without residual modes, both when the residual mode is based on a static distributed load on the deck (denoted “deck” in the plots in this chapter) or based on a static line load along the rails (denoted “pointload” in the plots in this chapter). The bending moment still converges at the cut-off frequency 30 Hz when a residual mode is included in the analysis. Convergence curves for the shear

force and the bending moment of the analyses with residual modes are shown in Figure 6.17-6.22.

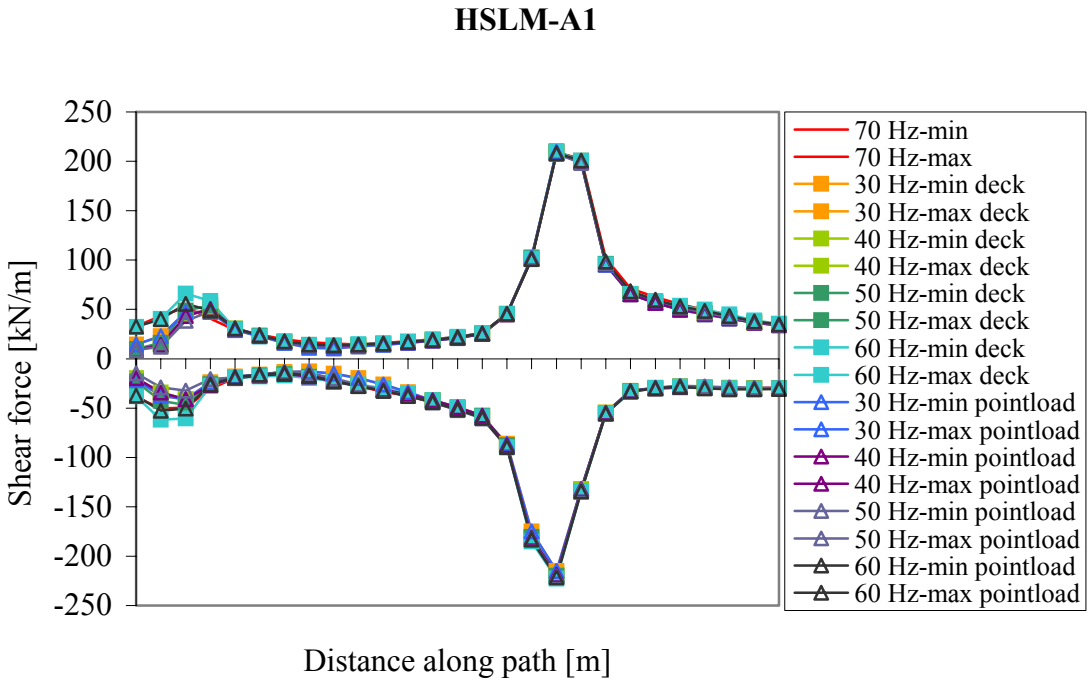

***Figure 6.17**: Maximum/minimum shear force from HSLM-A1 using different cut-off frequencies and including a residual mode.*

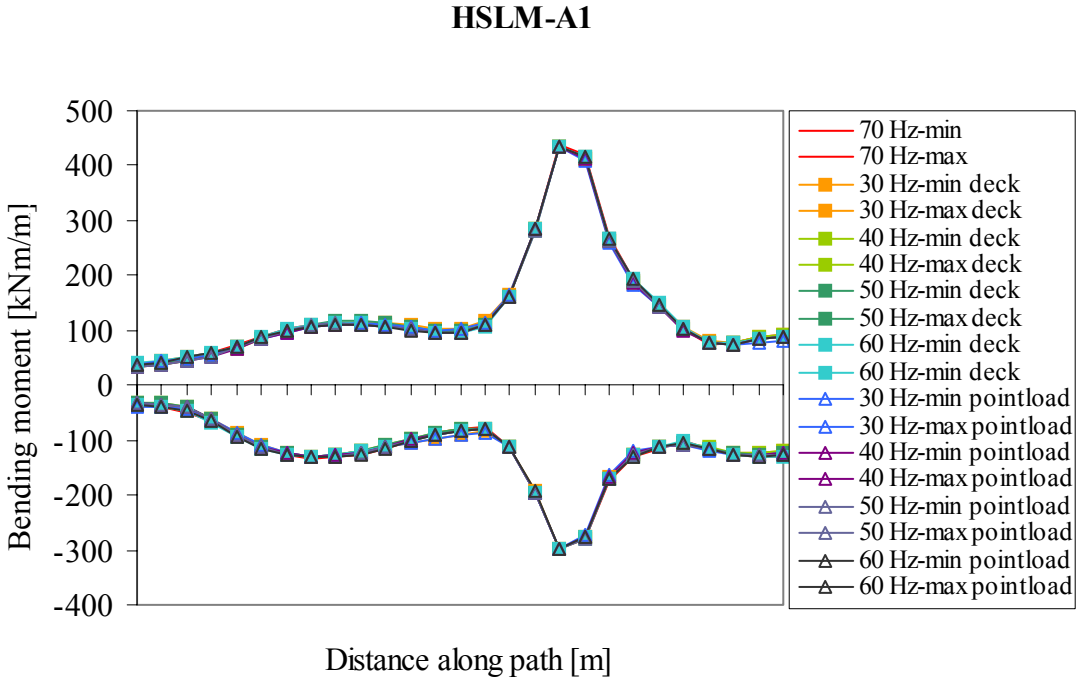

***Figure 6.18:** Maximum/minimum bending moment from HSLM-A1 using different cut-off frequencies and including a residual mode.*

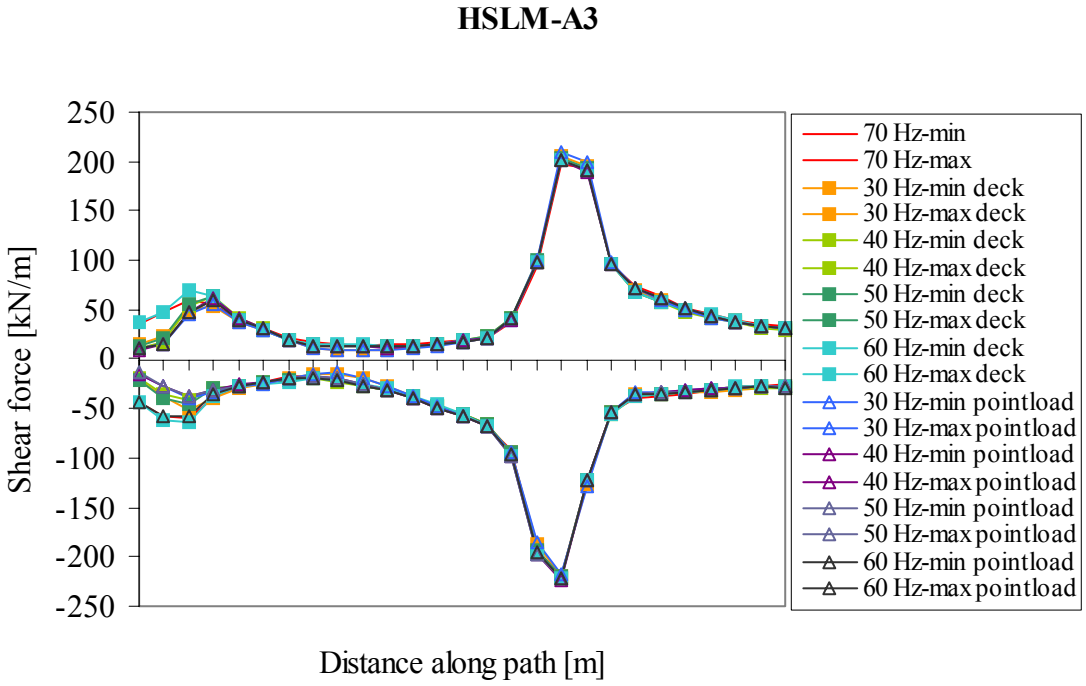

Figure 6.19: *Maximum/minimum shear force from HSLM-A3 using different cut-off frequencies and including a residual mode.*

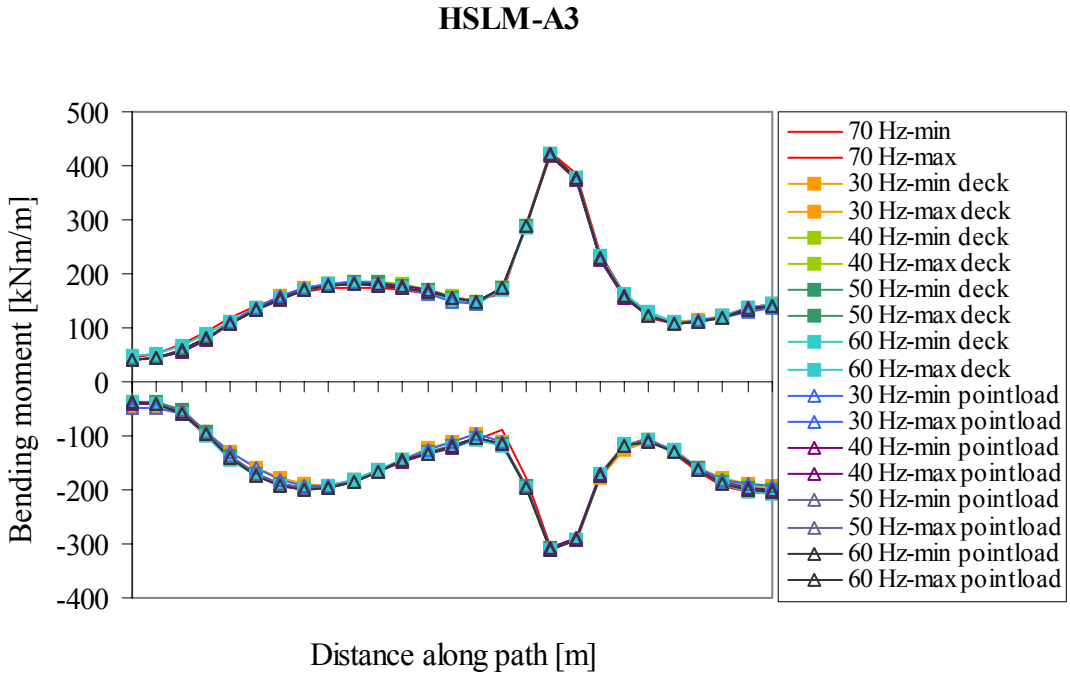

Figure 6.20: *Maximum/minimum bending moment from HSLM-A3 using different cut-off frequencies and including a residual mode.*

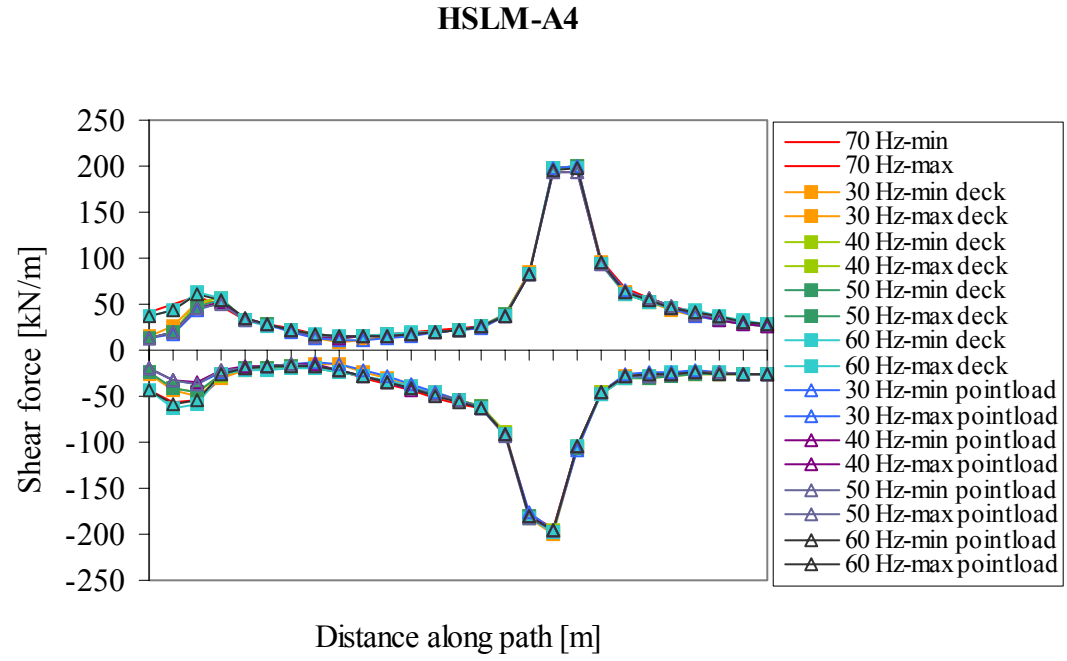

Figure 6.21: *Maximum/minimum shear force from HSLM-A4 using different cut-off frequencies and including a residual mode.*

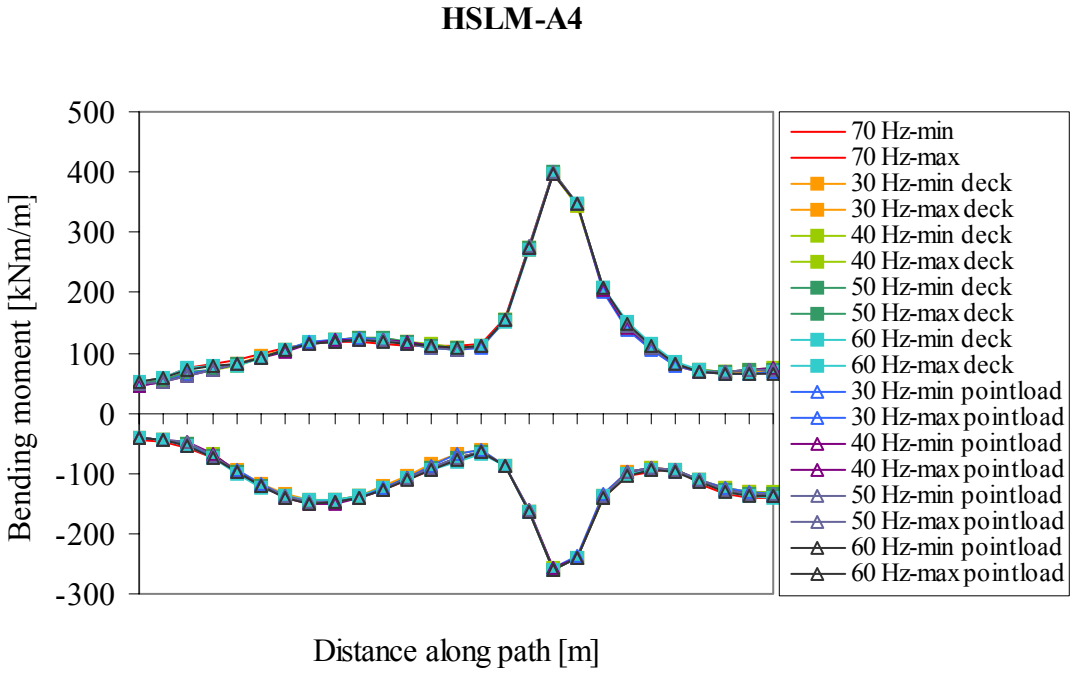

Figure 6.22*: Maximum/minimum bending moment from HSLM-A1 using different cut-off frequencies and including a residual mode.*

6.4.2 Bridge 2

For bridge 2, the residual mode seems to lower the cut-off frequency but only if the load used for the calculation of the residual mode shape is applied as point loads along the rails. Using that residual mode, the shear force converges at 80 Hz and the bending moment converges at 80 Hz. For analysis with the residual mode created from a distributed load on the deck, the shear force has not yet converged at the cut-off frequency 120 Hz. The same pattern can be seen for the bending moment, which has still not converged at 120 Hz. Convergence curves for the shear force and the bending moment are shown in Figure 6.23-6.26.

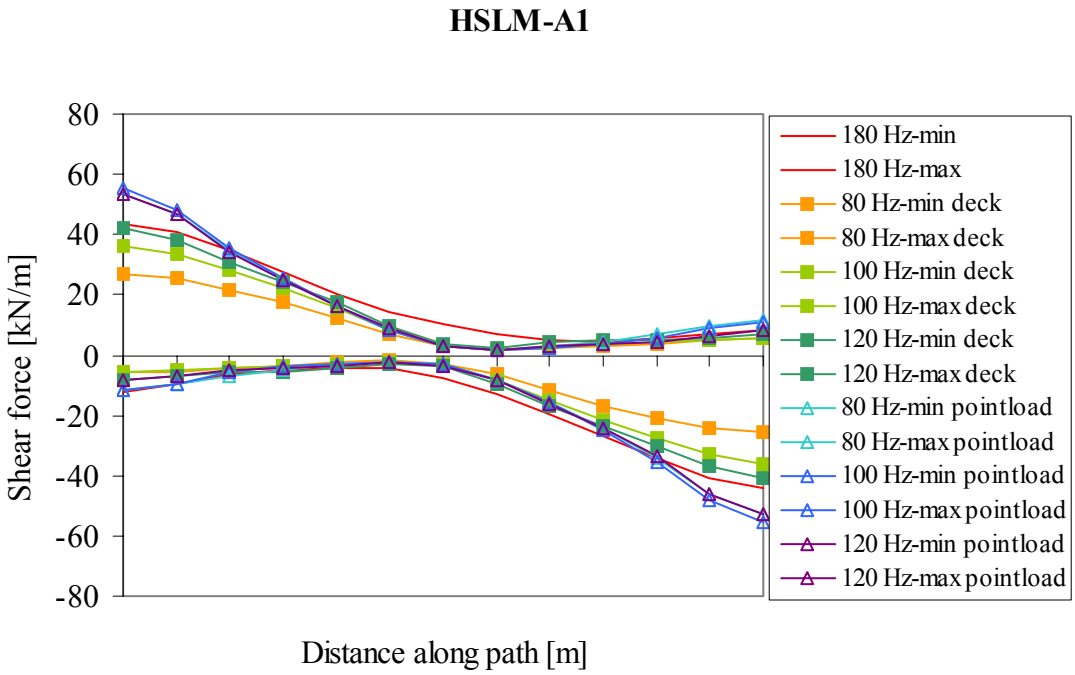

***Figure 6.23**: Maximum/minimum shear force from HSLM-A1 using different cut-off frequencies and including a residual mode.*

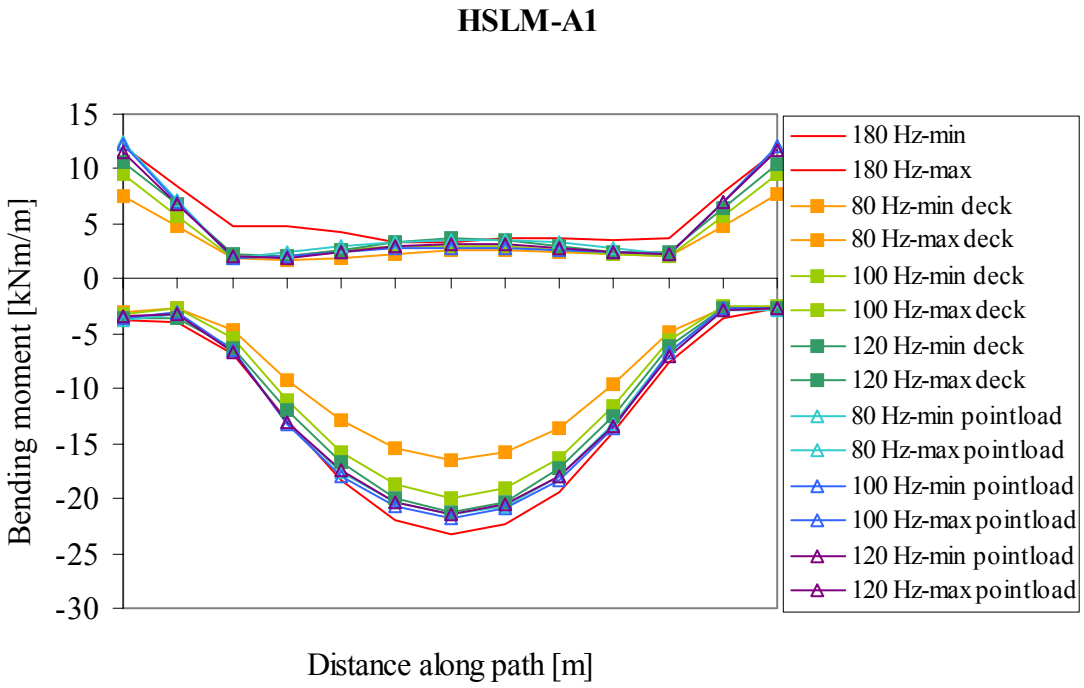

***Figure 6.24**: Maximum/minimum bending moment from HSLM-A1 using different cut-off frequencies and including a residual mode.*

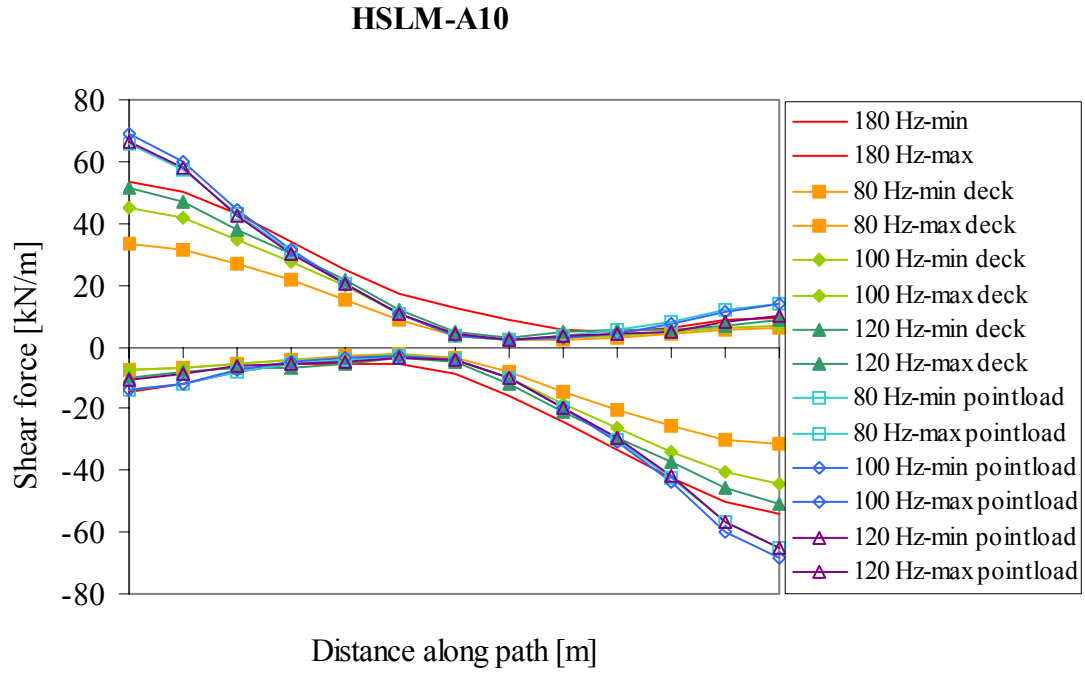

***Figure 6.25**: Maximum/minimum shear force from HSLM-A1 using different cut-off frequencies and including a residual mode.*

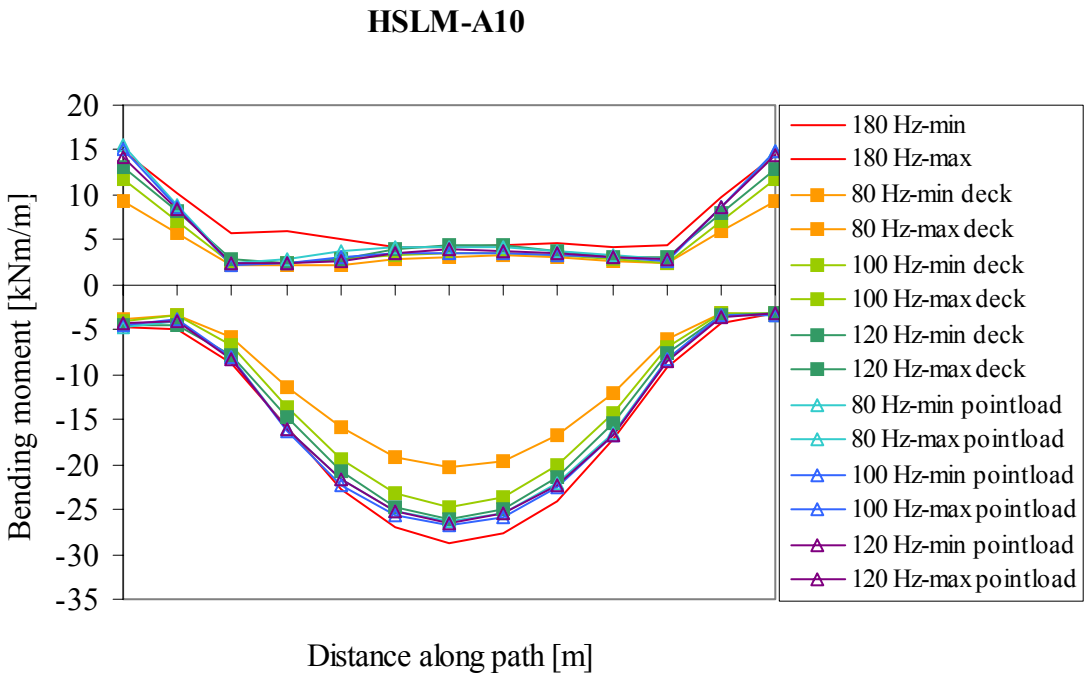

***Figure 6.26**: Maximum/minimum bending moment from HSLM-A1 using different cut-off frequencies and including a residual mode.*

The results regarding the cut-off frequencies when using residual modes for the two bridges are presented below. Table 6.6 shows the cut-off frequencies when the residual mode is shaped from a static distributed load added on the deck. Table 6.7 shows the cut-off frequencies when the residual mode is shaped from a static load applied along the rails as point loads. The following conclusions can be made:

- The shape of the residual mode is crucial for what impact it will have on the dynamic response. The shape of the residual mode is highly dependent on the shape of the load case in the static linear perturbation step preceding the extraction of the eigenmodes. Additionally, the shape and frequency of the residual mode is also dependent on the chosen cut-off frequency.
- Using residual modes when performing dynamic modal analyses on bridges can lower the cut-off frequency significantly, as can be seen in Table 6.6.

The effective mass in the structure at the cut-off frequencies, when using residual modes is shown in Table 6.8.

Bridge	Vehicle	Cut off frequencies regarding shear force		Cut off frequencies regarding bending moment		Chosen cut-off frequency with residual mode [Hz]
		Without residual mode [Hz]	With residual mode [Hz]	Without residual mode [Hz]	With residual mode [Hz]	
1	A1	60	60	30	30	60
1	A3	60	60	30	30	60
1	A4	60	60	30	30	60
2	A1	160	>120	160	>120	>120
2	A10	160	>120	160	>120	>120

***Table 6.6**: Cut-off frequencies at which the analyses converge for bridge 1 and 2 when residual modes, created from a static distributed load added on the deck, are included.*

Bridge	Vehicle	Cut off frequencies regarding shear force		Cut off frequencies regarding bending moment		Chosen cut-off frequency with residual mode [Hz]
		Without residual mode [Hz]	With residual mode [Hz]	Without residual mode [Hz]	With residual mode [Hz]	
1	A1	60	60	30	30	60
1	A3	60	60	30	30	60
1	A4	60	60	30	30	60
2	A1	160	80	160	80	80
2	A10	160	80	160	80	80

***Table 6.7**: Cut-off frequencies at which the analyses converge for bridge 1 and 2 when residual modes, created from a static load applied along the rails as point loads, are included.*

Bridge	Cut-off frequency	Effective mass when static load is applied on deck as a distributed load [%]	Effective mass when static load is applied along rails as point loads [%]
1	60	94	90
2	80	53	48

***Table 6.8**: Effective mass at the cut-off frequencies, when using a residual mode.*

7 Conclusions

For bridge 1 shear force and bending moment converged at 60Hz and 30 Hz respectively, when using a 10% convergence criterion. An appropriate cut-off frequency for the bridge would be 60 Hz when studying section forces. Bridge 2 on the other hand converged at 160 Hz for both the shear force and the bending moment and an appropriate cut-off frequency when studying the section forces is 160 Hz.

From these results three main conclusions can be made:

1. The type and geometry of the bridge is critical to which cut-off frequency needs to be chosen
2. The result components of section forces may converge at different cut-off frequencies.

3. Sections forces converge at the same frequency for all vehicles analysed, which means that a cut-off frequency for one vehicle can be used for all the remaining vehicles.

Since all vehicles seems to converge at the same cut-off frequency, it is possible to estimate the maximum cut-off frequency needed in the analyses by looking at the highest frequency that any of the 10 vehicles can generate. The cut-off frequency for bridge 2 is about 160 Hz. Very few bridges are stiffer than bridge 2. This indicates that a cut-off frequency four times the highest load frequency that any of the trains generate is satisfied ($4 \cdot 41.7 = 166.8$) for most concrete bridges. Choosing a cut-off frequency for analyses of larger bridges, like bridge 1, which does not need a high cut-off frequency, still requires further investigation.

Moreover, the results show that using residual modes in the analysis can be a great help to lower the cut-off frequency, especially for short and stiff bridges with high eigenfrequencies. For larger bridges, the residual mode might not be as helpful but at the same time, is innocuous to the results. To make the use of residual modes as helpful as possible, it is important to know how to design the static load case used for calculation of the mode shape. The solution of the static load case should be as similar to the dynamic load as possible. Of the two alternative load case shapes evaluated in this project, the best results were achieved when concentrated forces were applied along the rails.

The study shows, as expected, that effective mass is not an appropriate method to find cut-off frequencies when analysing bridges if the ground is assumed to be un-deformable. For bridge 2, the cut-off frequency is chosen to 160 Hz but by then, the effective mass in structure is only 56 % of the total mass. When using a residual mode, based on a static load created by point loads applied along the rails, the effective mass is even lower, about 48 % of the total mass that is able to move in the structure.

The following remarks should be regarded when making conclusions from the results:

- Dynamic modal analyses are sensitive when it comes to choosing a correct time increment size. If a rather moderate time increment is chosen a peek in the output may be lost as discussed in [3]. The time increment (*dt*) for the analyses presented in this paper is chosen as $dt=1/(f_{max}\cdot 10)$, where f_{max} is the cut-off frequency used in the analysis. To investigate if a poor time increment was used, which caused a non-converge for analyses using lower cut-off frequencies, a test was performed on bridge 2. An analysis with a cut-off frequency of 100Hz with the time increment $dt=1/(120\cdot 10)$ was carried out. The "original" analysis were run with a $dt=1/(100\cdot 10)$. The results varied about 2 % from the analysis with time increment $dt=1/(100\cdot 10)$ but about 20 % from the results of the analysis with cut-off frequency 120 Hz ($dt=1/(120\cdot 10)$). The time increment of $1/(f_{max}\cdot 10)$ was therefore considered to be satisfying.

- When the modal base is increased the peek response (e.g. the shear fore) might be slightly displaced on the speed-axel in a speed-response diagram [3]. The analyses in this project have been carried out with a speed increment of 5 km/h that is required [2]. It is therefore possible that a part of the difference in response between two analyses only with different cut-off frequencies (and therefore different time increment) is due to a dislocation of the speed at which the response peeked. This is a reason not to be too conservative when setting up a required convergence requirement.

- A clear indication revealing the need of more investigation on this topic is the fact that the result file for bridge 1, using a cut-off frequency of 70 Hz, was not possible to open when first tested. The ABAQUS support was contacted but the problem was not solved in the timeframe of this project. What caused the problem was not clarified but it seems to be related to the size of the result file, which was relatively large, around 7.5 GB. Splitting the analysis into two solved the problem. If the size of the result file was in fact the problem, narrow guidelines pointing towards the "right" cut-off frequency becomes even more important.

- Nodes connected to the ground have been locked in all degrees of freedom in both models. This is an assumption that is allowed according to Banverket, the Swedish railway authority. The alternative is to take the elastic deformation of the soil into account. This could lower the eigenfrequencies of the first bending modes for the bridges because of the stiffness reduction. The following vertical bending modes will also have a lower eigenfrequency and from experience the vertical bending modes affect the results at great extent. For bridge 1 the difference would probably be smaller. For bridge 2, the effect of letting the bridge interact with the ground would probably be quite significant since a relatively large ratio of the bridge mass is connected to the ground. If the eigenfrequencies of the vertical bending modes are lowered when the elastic deformation of the soil is taken into account, it would probably lead to a lower cut-off frequencies when performing the kind of analyses carried out in this project.

- Bridge 1 might converge earlier with respect to the bending moment, than revealed in this paper. No analyses were made with lower cut-off frequency than 30 Hz.

- Note that some convergence plots might not have converged in every point even though they are said to fulfil the convergence criterion. The section forces are used when dimensioning the reinforcement of the bridges and the different aspects mentioned in 4.4.2 can be used to determine that the analysis still converge at a certain cut-off frequency.

8 Further work

More convergence studies should be made for a larger number of bridges and other types of bridges, in order to be able to form narrower guidelines for the choice of a suitable cut-off frequency. It would be interesting to perform more analyses on one bridge type, for example a three span bridge. Perhaps a relation between for example, the span lengths of one bridge type and the cut-off frequency can be found with a wider result basis. In addition, more analyses including more vehicles (trains) should be performed to be able to determine further conclusions about the effect that different types of vehicles have on the cut-off frequency.

The effects of residual modes need to be further investigated. The residual modes are still not perfectly created to compensate for all the truncated modes. Perhaps one alternative, which was not investigated in this report, is to use multiple residual modes for each analysis instead of a single residual mode.

Furthermore, if the interaction properties between the bridge and ground can be established the bridges could be modelled to that respect. Today the interaction is not modelled. Instead, fixed support is used in the nodes where the bridge is in contact with the ground. The fix support leads to stiff bridge models that result in higher eigenmodes, opposed to when the interaction with the ground is taken in into account. Moreover, the models would then be more similar to the reality and thus the results could then be even more reliable than they are today.

References

[1] Niels Saabye Ottosen and Hans Petersson, *Introduction to the Finite Element Method*, Prentice Hall, 1992

[2] Banverket, BV BRO – Banverkets ändringar och tillägg till Vägverkets Bro, 2004, Utgåva 7. BVS 583.10, 2004

[3] Lena Björklund, *Dynamic Analysis of a Railway Bridge subjected to High Speed Trains*, Master of Science Thesis, Royal Institute of Technology, Stockholm, 2005

[4] ABAQUS Online Documentation, version 6.6

[5] Scanscot Technology AB, Teknisk Rapport 97404/TR-01, *BDL – Delprojekt Analys - Bestämning av cut-off frekvens*, 1997

[6] ASCE, *Seismic Design Criteria for Structures, Systems, and Components in Nuclear Facilities*, ASCE/SEI 43-05 American Society of Civil Engineers, 2005

[7] Spanne Sven, *Lineära system*, 4th edition, Lund, 1997

[8] Ray W. Clough and Joseph Penzien, *Dynamics of Structures*, McGraw-Hill, 1982

Appendix A

The most important eigenmodes and eigenfrequencies of bridge 1:

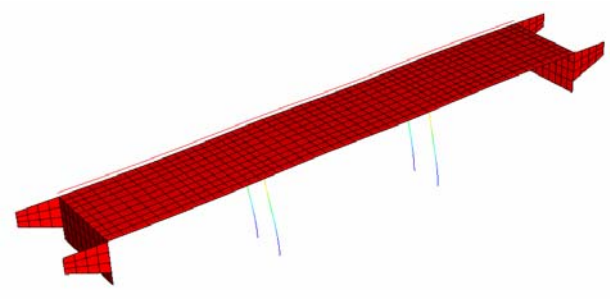

Eigenmode 1: 2.11 Hz

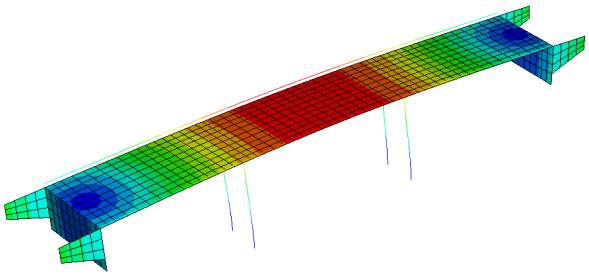

Eigenmode 2: 6.95 Hz

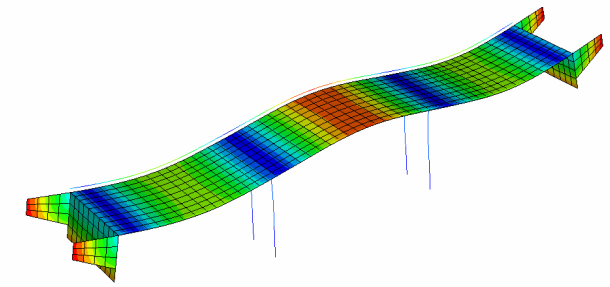

Eigenmode 3: 8.55 Hz

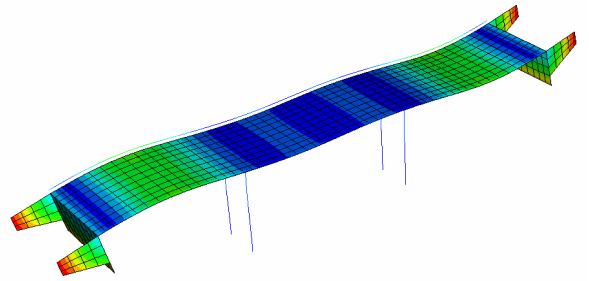

Eigenmode 4: 11.20 Hz

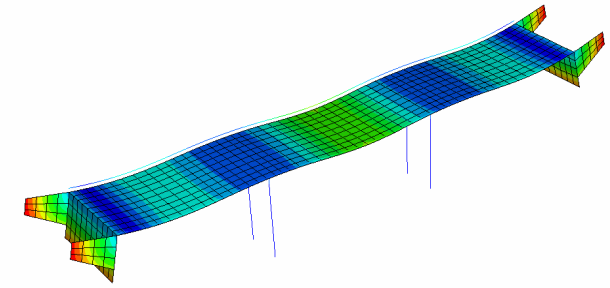

Eigenmode 5: 13.79 Hz

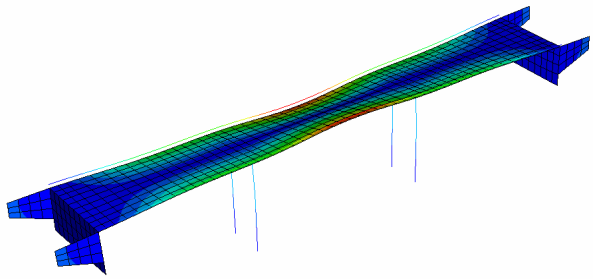

Eigenmode 6: 16.32 Hz

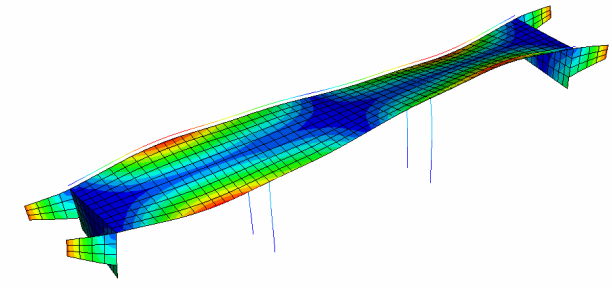

Eigenmode 7: 20.62 Hz

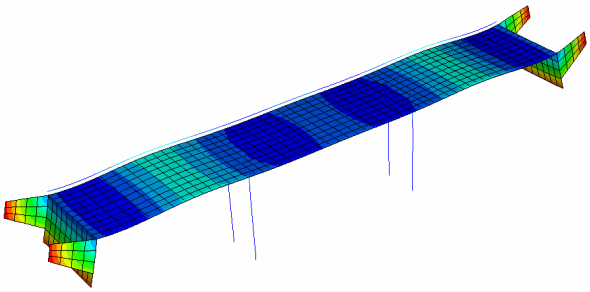

Eigenmode 8: 20.86 Hz

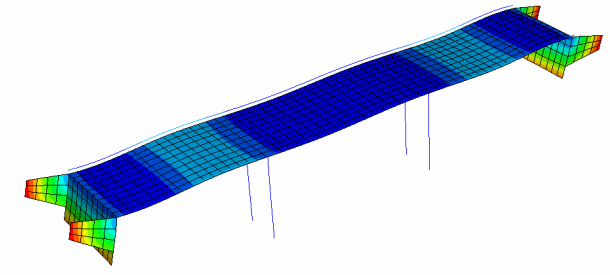

Eigenmode 9: 20.99 Hz

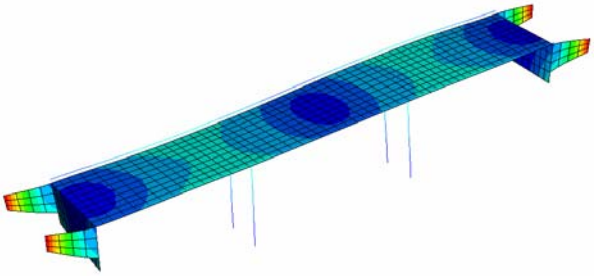

Eigenmode 10: 22.18 Hz

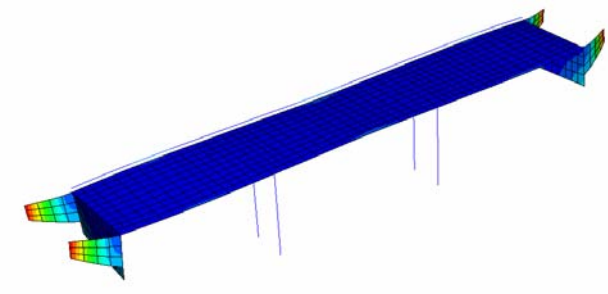

Eigenmode 11: 24.14 Hz

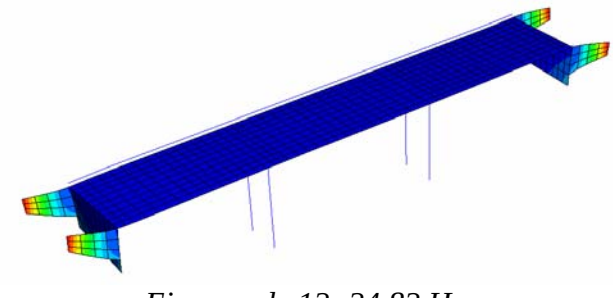

Eigenmode 12: 24.82 Hz

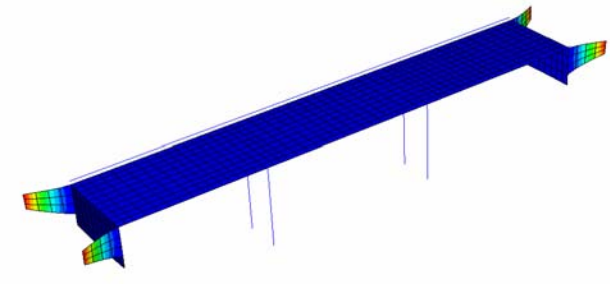

Eigenmode 13: 25.08 Hz

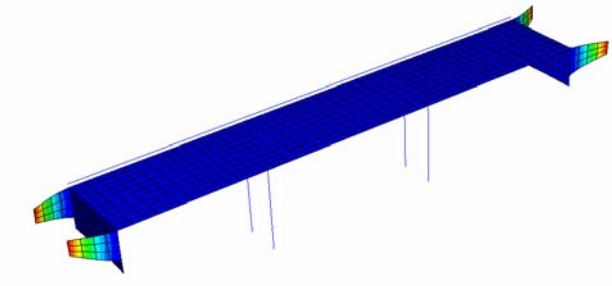

Eigenmode 14: 25.08 Hz

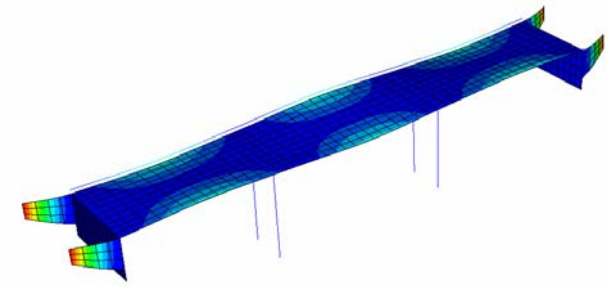

Eigenmode 15: 25.48 Hz

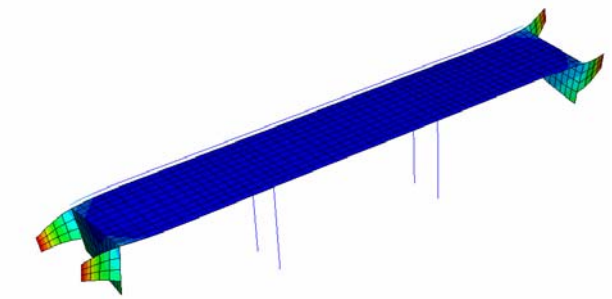

Eigenmode 16: 26.34 Hz

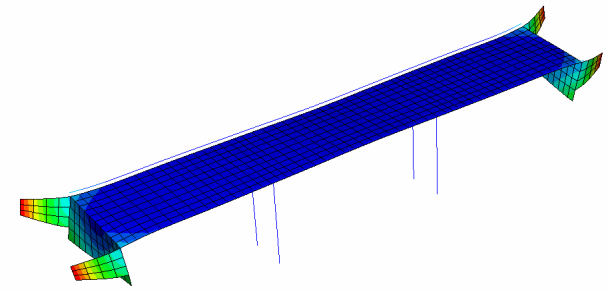

Eigenmode 17: 26.40 Hz

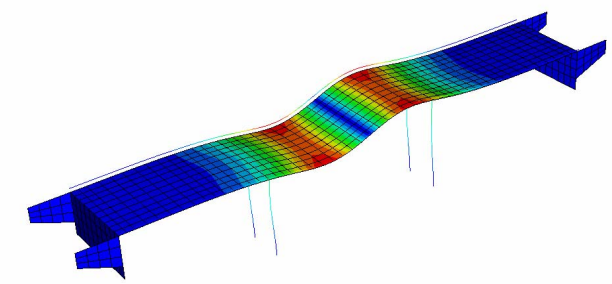

Eigenmode 18: 26.47 Hz

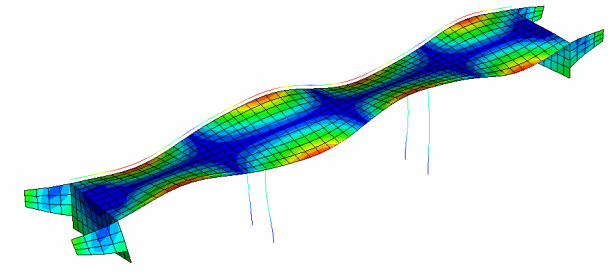

Eigenmode 19: 34.40 Hz

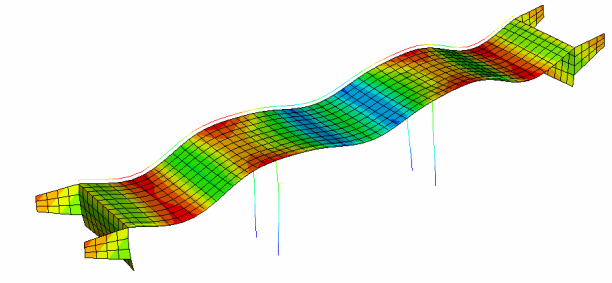

Eigenmode 20: 35.61 Hz

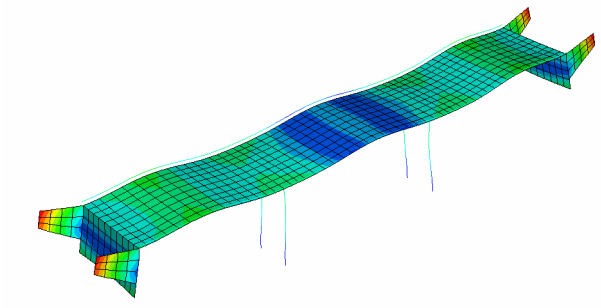

Eigenmode 21: 37.95 Hz

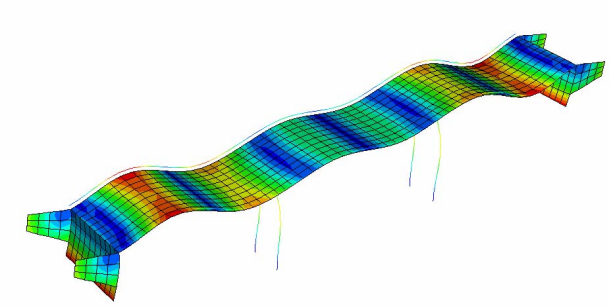

Eigenmode 22: 39.13 Hz

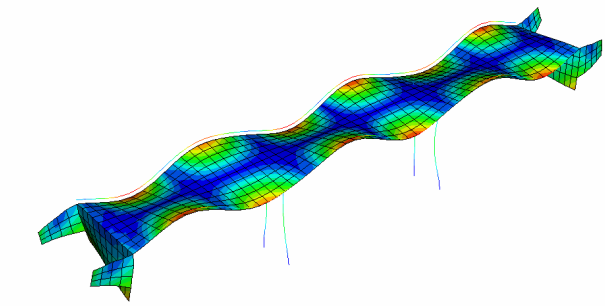

Eigenmode 37: 55.87 Hz

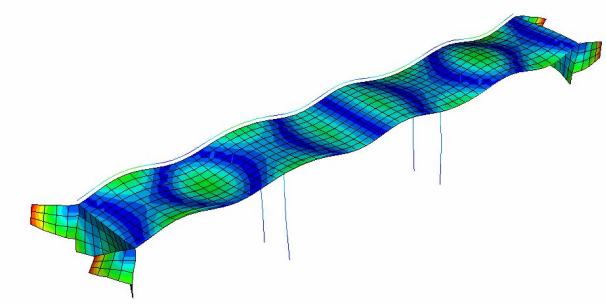

Eigenmode 41: 65.34 Hz

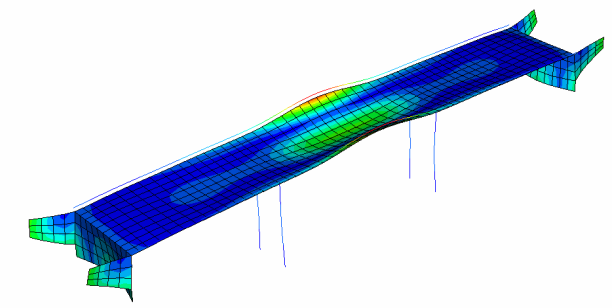

Eigenmode 42: 65.84 Hz

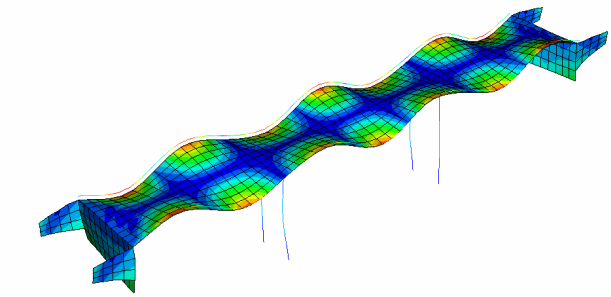

Eigenmode 43: 67.11 Hz

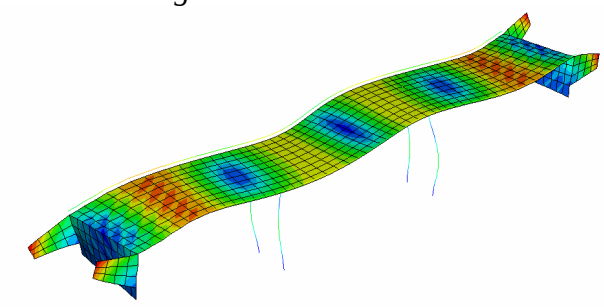

Eigenmode 44: 68.29 Hz

Appendix B

The most important eigenmodes and eigenfrequencies of bridge 2:

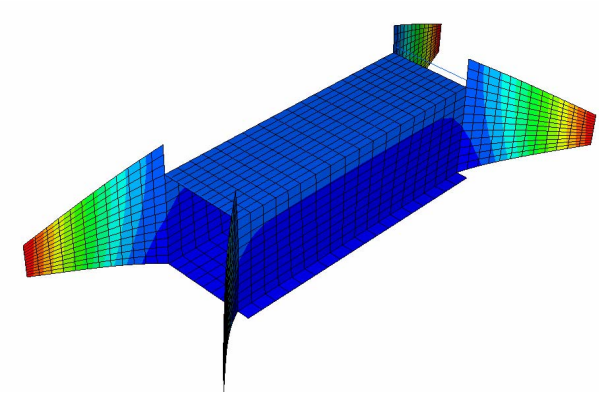

Eigenmode 1: 11.40 Hz

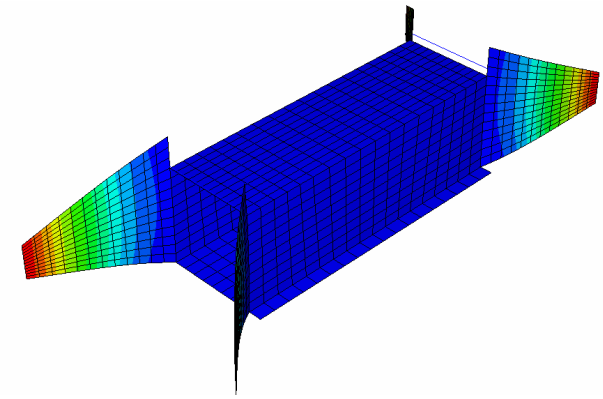

Eigenmode 2: 11.75 Hz

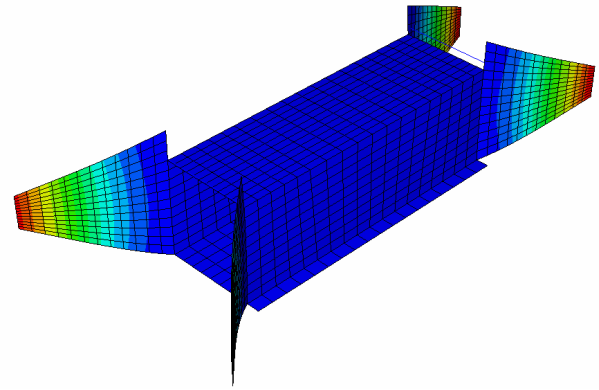

Eigenmode 3: 11.96 Hz

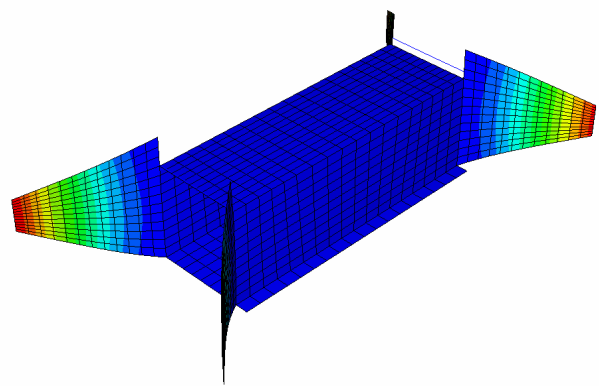

Eigenmode 4: 11.96 Hz

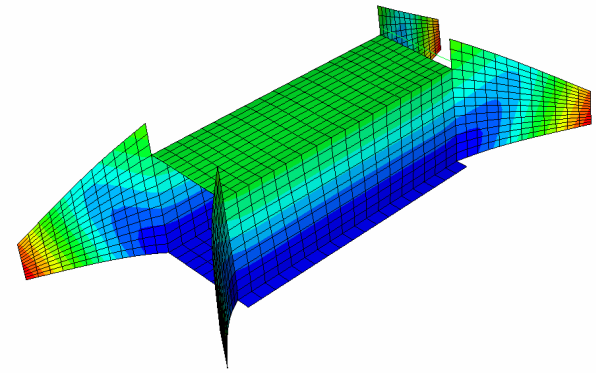

Eigenmode 5: 14.94 Hz

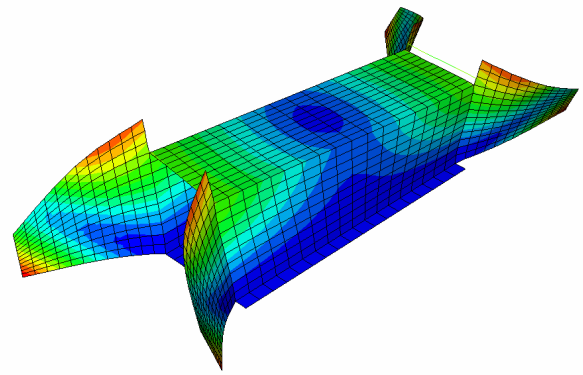

Eigenmode 6: 31.92 Hz

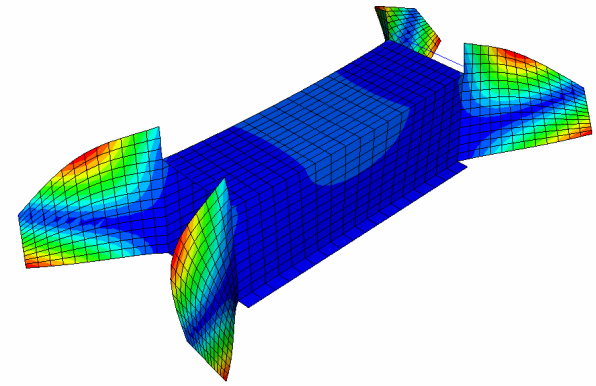

Eigenmode 7: 47.87 Hz

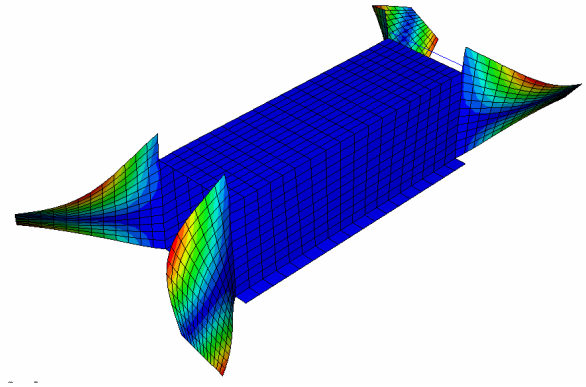

Eigenmode 8: 49.13 Hz

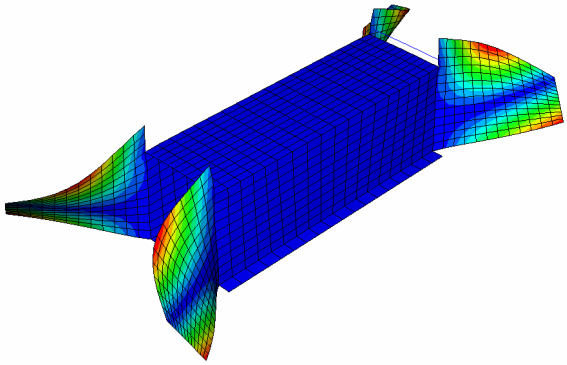

Eigenmode 9: 49.24 Hz

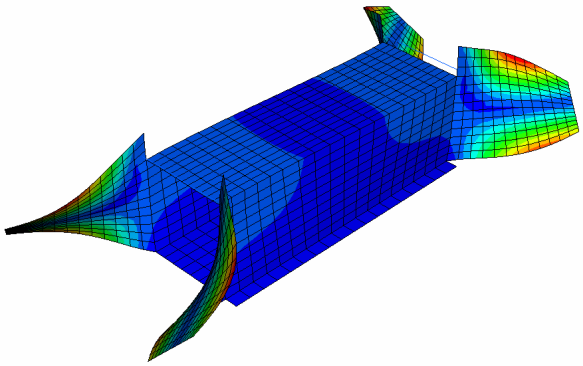

Eigenmode 10: 52.68 Hz

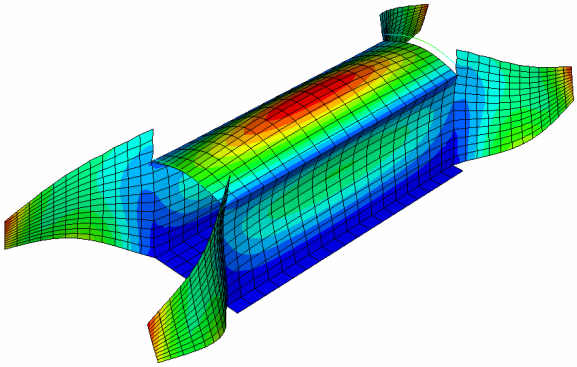

Eigenmode 16: 61.97 Hz

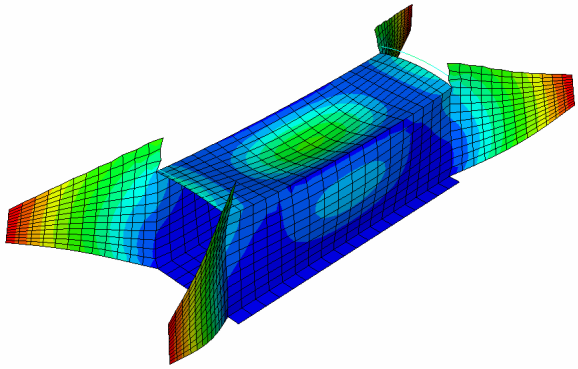

Eigenmode 17: 66.47 Hz

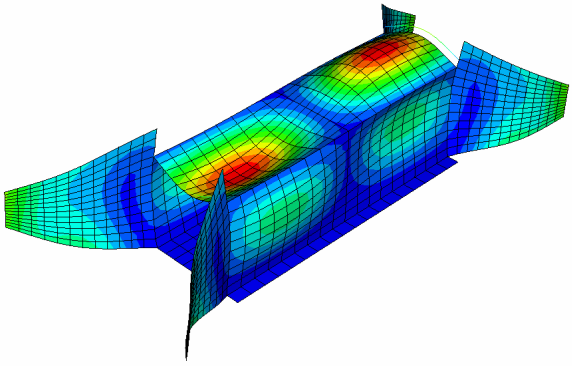

Eigenmode 18: 70.39 Hz

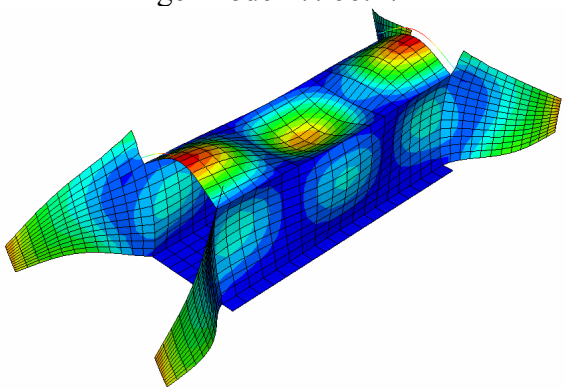

Eigenmode 21: 81.05 Hz

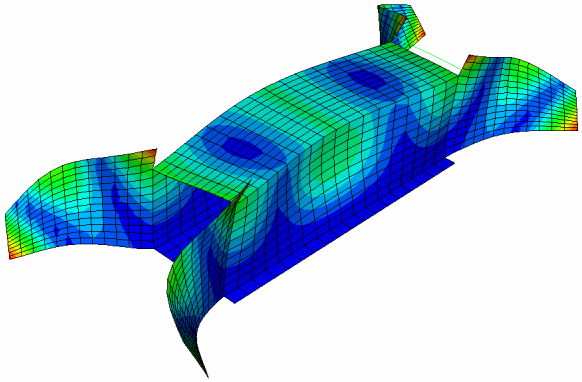

Eigenmode 22: 82.58 Hz

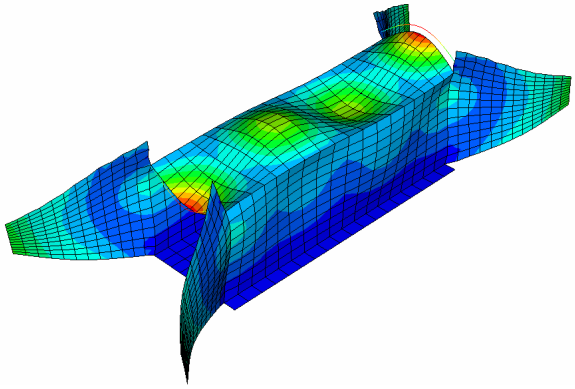

Eigenmode 24: 95.12 Hz

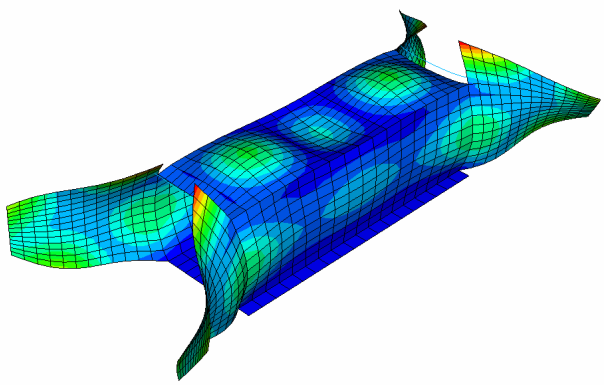

Eigenmode 27: 106.79 Hz

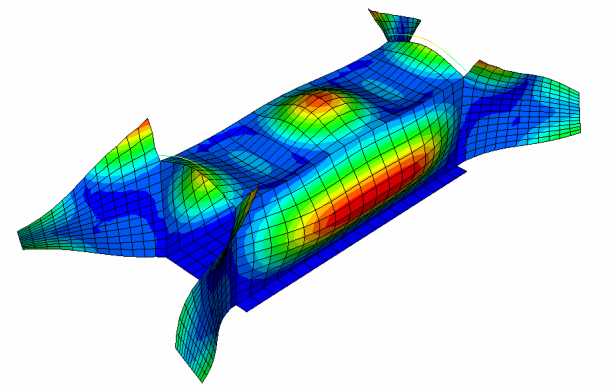

Eigenmode 29: 113.02 Hz

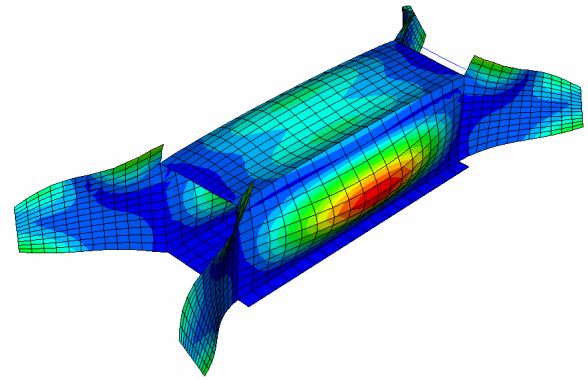

Eigenmode 30: 114.85 Hz

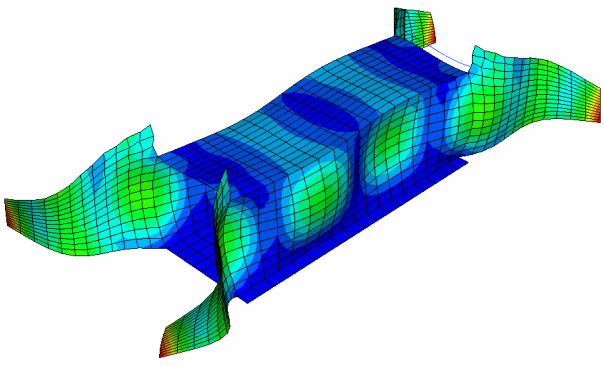

Eigenmode 33: 118.55 Hz